Conformational Analysis of Poly(trimethylene imine) and Poly(*N*-methyltrimethylene imine) by the Rotational Isomeric State Scheme with up to Fourth-Order Intramolecular Interactions

Yuji Sasanuma,* Fumiko Teramae, Hiroki Yamashita, Ippei Hamano, and Satoshi Hattori

Department of Applied Chemistry and Biotechnology, Faculty of Engineering, Chiba University, 1-33 Yayoi-cho, Inage-ku, Chiba 263-8522, Japan

Received January 21, 2005; Revised Manuscript Received February 13, 2005

ABSTRACT: An inversional-rotational isomeric state (IRIS) scheme including first-order to fourth-order intramolecular interactions has been developed and applied to conformational analysis of poly(trimethylene imine) (PTMI) and poly(*N*-methyltrimethylene imine) (PMTMI). Bond conformations and conformational energies of PTMI and PMTMI were evaluated from ab initio molecular orbital calculations at the MP2/6-311++G(3df, 3pd)//HF/6-31G(d) level and ^{1}H and ^{13}C NMR experiments for the monomeric model compounds, $CH_3NR_1CH_2CH_2CH_2NR_2CH_3$ ($R_1 = R_2 = H$; $R_1 = H$ and $R_2 = CH_3$; $R_1 = R_2 = CH_3$). The IRIS analysis yielded the following data on the polymers at 25 °C: the characteristic ratio for the infinite chain, 3.5 (PTMI) and 4.2 (PMTMI); trans fractions of the C−C and C−N bonds, respectively, 0.29 and 0.77 (PTMI) and 0.40 and 0.65 (PMTMI); the *meso*-diad probability, 0.44 (PTMI) and 0.48 (PMTMI). Intramolecular hydrogen bonds were found in the polyimines: PTMI, N−H···N (the interaction energy, −0.83 kcal mol^{-1}) and C−H···N (−0.15 kcal mol^{-1}); PMTMI, C−H···N (−0.40 kcal mol^{-1}). The chain dimension, stereochemical configuration, and bond conformations of the polyimines are sensitive to the first-order interaction energy around the C−C bond and the hydrogen-bond energies. Polar solvents weaken the hydrogen bonds to increase the chain dimension and randomize the configuration.

1. Introduction

In a previous paper,[1] we have described conformational characteristics of poly(ethylene imine) (PEI, $[-CH_2CH_2NH-]_x$). The PEI chain exhibits inversional and rotational isomerizations; the conformation and configuration are averaged to be observed. For the conformational analysis, we have developed a methodology based on the statistical mechanics for chain molecules,[2,3] i.e., an inversional-rotational isomeric state (IRIS) scheme. The PEI chain forms two types of intramolecular N−H···N hydrogen bonds, which cause a strong gauche preference of the C−C bond and hence shrink the polymeric chain. In polar solvents, the hydrogen bonds are partly switched to polymer···solvent interactions. This transfer expands the PEI chain considerably and randomize the configuration.

In the present study, we have treated poly(trimethylene imine) (PTMI, $[-CH_2CH_2CH_2NH-]_x$). Linear PTMI has been synthesized by ring-opening polymerization of unsubstituted and 2-substituted 5,6-dihydro-4*H*-1,3-oxazines and subsequent hydrolysis of the resultant polymers.[4−9] The mechanism of the polymerization has been investigated in detail. However, only scant information on structures and physical properties of PTMI has been obtained.[10] In this study, we have attempted to characterize the conformation and solution properties of PTMI. The N−C−C−C−N unit corresponds to one generation of poly(trimethylene imine) dendrimers.[11−14] Because the dendrimers perfectly branch at the nitrogen site, poly(*N*-methyltrimethylene imine) (PMTMI, $[-CH_2CH_2CH_2N(CH_3)-]_x$) may be a more appropriate model for PTMI dendrimers than PTMI. This paper also deals with PMTMI.

* To whom correspondence should be addressed. E-mail: sasanuma@faculty.chiba-u.jp FAX +81 43 290 3394.

As model compounds of PTMI and PMTMI, *N,N′*-dimethyl-1,3-propanediamine (di-MPDA), *N,N,N′*-trimethyl-1,3-propanediamine (tri-MPDA), and *N,N,N′,N′*-tetramethyl-1,3-propanediamine (tetra-MPDA) have been adopted to evaluate the bond conformations and conformational energies from ab initio molecular orbital (MO) calculations and NMR experiments (see Figure 1). The conformational energies thus established were applied to the IRIS scheme to calculate the chain dimensions, diad probabilities, and bond conformations. The N−H···H−N, N−H···lone pair, and lone pair···lone pair contacts of PTMI, depending on internal rotations around four bonds, N−C−C−C−N, must be treated as fourth-order interactions. Here, the IRIS scheme including up to fourth-order interactions has been systematically formulated and applied to PTMI.

2. MO Computations and NMR Experiments

2.1. Ab Initio MO Calculations. Ab initio MO calculations were carried out with the Gaussian98 program[15] installed on an HPC−P4L or an HPC−IAXP8 computer. For each conformer of di-MPDA, tri-MPDA, and tetra-MPDA, the geometrical parameters were fully optimized at the HF/6-31G(d) level, and the thermal correction to the Gibbs free energy (at 25 °C) was calculated with a calibration factor of 0.9135.[16] With the optimized geometry, the self-consistent field (SCF) energy was computed at the MP2/6-311++G(3df, 3pd) level. The Gibbs free energy (G_k, k: conformer) was evaluated from the SCF energy and thermal-correction term. In this paper, the free energy is given as the value relative to a specified conformer and denoted as ΔG_k. For comparison with experiment, NMR coupling constants of 2-methylpiperidine (2MPD) were calculated at the HF/6-311+G(2d, p)//HF/6-31G(d) and B3LYP/6-311+G(2d, p)//B3LYP/6-31G(d) levels with the Gaussian03W program.[17]

2.2. NMR Measurements. ^{1}H (^{13}C) NMR spectra were measured at 500 MHz (125.65 MHz) on a JEOL JNM-LA500

10.1021/ma050130y CCC: $30.25
Published on Web 03/23/2005

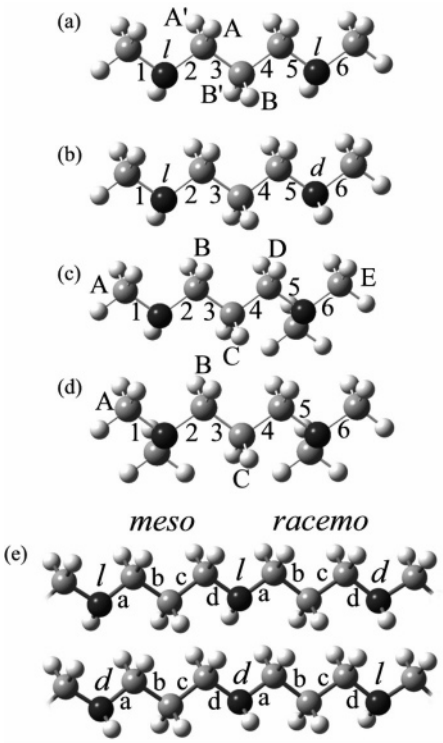

Figure 1. All-trans states of (a) *meso* (*ll*) *N,N′*-dimethyl-1,3-propanediamine (di-MPDA), (b) *racemo* (*ld*) di-MPDA, (c) *N,N,N′*-trimethyl-1,3-propanediamine (tri-MPDA), (d) *N,N,N′,N′*-tetramethyl-1,3-propanediamine (tetra-MPDA), and (e) poly(trimethylene imine) (PTMI). As indicated, the bonds and atoms are designated. The *l* and *d* forms are defined as follows. For example, the di-MPDA molecule in the all-trans state is put on paper as shown. When the hydrogen atom of the left-hand NH group appears on this (that) side of the paper, the nitrogen site is considered to adopt the *d* (*l*) form. For other nitrogen sites, the *d* and *l* configurations are defined similarly. The *dd* and *ll* forms are referred to as *meso*, and *dl* and *ld* as *racemo*. In this paper, the *meso* and *racemo* forms are represented mainly by the *ll* and *ld* isomers, respectively. The all-trans *meso* and *racemo* forms have the two NH hydrogen atoms on the same and opposite sides, respectively. If the NH hydrogen atoms of PTMI are replaced by methyl groups, the resultant polymer corresponds to poly(*N*-methyltrimethylene imine) (PMTMI).

spectrometer equipped with a variable temperature controller in the Chemical Analysis Center of Chiba University. During the measurement the probe temperature was maintained within ± 0.1 °C fluctuations. The $\pi/2$ pulse width, data acquisition time, and recycle delay were 5.6 (5.0) μs, 13.1 (2.0) s, and 3.7 (2.0) s, respectively. Here, the values in the parentheses represent the ^{13}C NMR parameters. The gated decoupling technique was used in the ^{13}C NMR measurements.

The model compounds, di-MPDA, tri-MPDA, tetra-MPDA, and 2MPD, were purchased from Aldrich or Tokyo Kasei Kogyo and used without further purification. The solvents were cyclohexane-d_{12}, chloroform-*d*, dimethyl-d_6 sulfoxide (DMSO-d_6), methanol-d_4, and deuterium oxide, and the solute concentration was ca. 5 vol %. The aqueous solutions were fully basic. For example, pH of the deuterium oxide solution of di-MPDA was estimated as ca. 12.[18]

3. Results and Discussion

3.1. ^{1}H NMR. Parts a and b of Figure 2 show ^{1}H NMR spectra observed from di-MPDA in cyclohexane-d_{12} and methanol-d_4, respectively. Simulations using the gNMR program[27] yielded vicinal coupling constants, $^3J_{HH}$ (=$^3J_{AB}$ = $^3J_{A'B'}$) and $^3J'_{HH}$ (=$^3J_{AB'}$ = $^3J_{A'B}$), as listed in

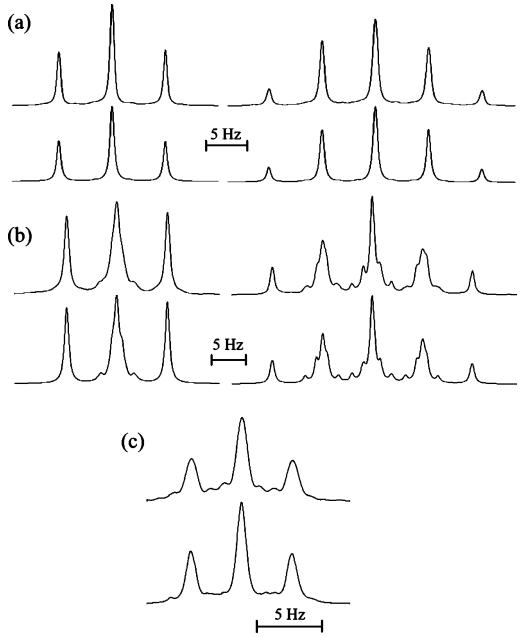

Figure 2. ^{1}H NMR spectra of methylene protons, A and A′ (left) and B and B′ (right), of di-MPDA dissolved in (a) cyclohexane-d_{12} and (b) methanol-d_4 at 25 °C. (c) ^{13}C NMR spectra of methyl carbons of di-MPDA in chloroform-*d* at 25 °C. The observed and calculated spectra are shown above and below, respectively. For designations of the protons, see Figure 1.

Table 1. Observed Vicinal ^{1}H−^{1}H and ^{13}C−^{1}H Coupling Constants of di-MPDA

solvent	temp (°C)	$^3J_{HH}$ (Hz)	$^3J'_{HH}$ (Hz)	$^3J_{CH}$ (Hz)
cyclohexane-d_{12}	15	6.01	6.84	3.68
	25	6.02	6.86	3.75
	35	6.05	6.87	3.78
	45	6.10	6.86	3.82
	55	6.13	6.88	3.84
chloroform-*d*	15	6.56	7.40	3.66
	25	6.53	7.37	3.72
	35	6.51	7.35	3.75
	45	6.52	7.32	3.82
	55	6.42	7.35	3.86
dimethyl-d_6 sulfoxide	15	6.54	7.34	3.69
	25	6.54	7.34	3.74
	35	6.51	7.31	3.79
	45	6.51	7.31	3.83
	55	6.49	7.29	3.89
methanol-d_4	15	5.99	8.81	3.91
	25	6.02	8.72	3.96
	35	6.02	8.66	4.00
	45	6.09	8.54	4.06
	55	6.10	8.47	4.08
deuterium oxide	15	6.12	8.58	3.48
	25	6.08	8.65	3.57
	35	6.07	8.64	3.62
	45	6.07	8.60	3.68
	55	6.06	8.59	3.81

Table 1. The observed vicinal coupling constants can be expressed as

$$^3J_{HH} = {}^3J_G^{HH} p_t^{CC} + \frac{{}^3J_T'^{HH} + {}^3J_G''^{HH}}{2} p_g^{CC} \qquad (1)$$

and

$$^3J'_{HH} = {}^3J_T^{HH} p_t^{CC} + \frac{{}^3J_G'^{HH} + {}^3J_G'''^{HH}}{2} p_g^{CC} \qquad (2)$$

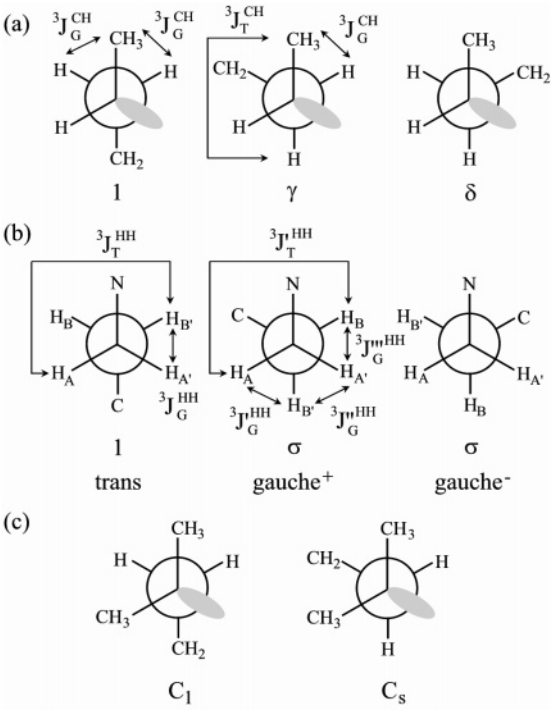

Figure 3. Conformations around the (a) NH−CH_2, (b) CH_2 −CH_2, and (c) CH_2 −N(CH_3) bonds with definitions of vicinal coupling constants. The Greek letters represent first-order interactions of di-MPDA and PTMI.

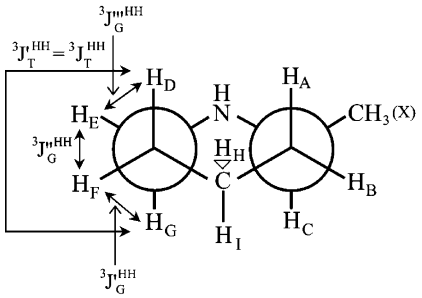

Figure 4. 2-Methylpiperidine (2MPD). The hydrogen atoms are designated as indicated. The vicinal coupling constants of 2MPD were used in the ^{1}H NMR analysis of eqs 1 and 2.

where $^3J_T^{HH}$s and $^3J_G^{HH}$s are defined in Figure 3, and p_t^{CC} and p_g^{CC} are trans and gauche fractions of the C−C bond, respectively. Therefore, we have

$$p_t^{CC} + p_g^{CC} = 1 \tag{3}$$

As $^3J^{HH}$s in eqs 1 and 2, we have used those observed from the N−CH_2 −CH_2 −CH_2 bond sequence of 2MPD (Figure 4); the 2-methyl substituent prevents the piperidine ring from flip-flopping. Figure 5 shows observed and calculated ^{1}H NMR spectra of 2MPD. In Table 2, the vicinal coupling constants are listed, together with the MO calculations. The p_t^{CC} and p_g^{CC} values were derived from eqs 1 and 2, and divided by their sum to satisfy eq 3, as in previous studies.[1,28] The trans fraction largely depends on solvent (Table 3); the solvent polarity induces the trans preference.

Figures 6 and 7 show ^{1}H NMR spectra observed from methylene groups of tri-MPDA and tetra-MPDA, respectively. The $^3J_{HH}$ and $^3J'_{HH}$ values of these compounds are given in the Supporting Information. The p_t^{CC} values, derived as above, are listed in Table 4. For

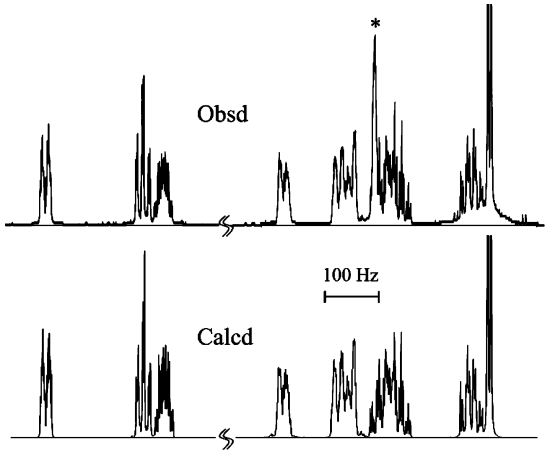

Figure 5. Observed and calculated ^{1}H NMR spectra of 2MPD dissolved in cyclohexane-d_{12} at 25 °C. The NMR parameters were determined as follows (δ in ppm and J in Hz): $\delta_A - \delta_X = 0.067$, $\delta_B - \delta_X = 0.553$, $\delta_C - \delta_X = 1.562$, $\delta_D - \delta_X = 0.390$, $\delta_E - \delta_X = 1.994$, $\delta_F - \delta_X = 0.505$, $\delta_G - \delta_X = 1.637$, $\delta_H - \delta_X = 0.755$, $\delta_I - \delta_X = 0.338$, $^2J_{AB} = -12.80$, $^3J_{AC} = 10.60$, $^3J_{AH} = 3.95$, $^3J_{AI} = 12.60$, $^3J_{BC} = 2.56$, $^4J_{BF} = 1.50$, $^3J_{BH} = 3.14$, $^3J_{BI} = 3.88$, $^3J_{CX} = 6.23$, $^3J_{DE} = 4.20$, $^2J_{DF} = -12.65$, $^3J_{DG} = 11.89$, $^3J_{DH} = 3.79$, $^3J_{DI} = 12.95$, $^3J_{EF} = 2.38$, $^2J_{EG} = -11.39$, $^4J_{EH} = 1.77$, $^3J_{FG} = 2.70$, $^3J_{FH} = 2.84$, $^3J_{FI} = 3.82$, and $^2J_{HI} = -13.59$. For designations of the protons, see Figure 4. The asterisk indicates a peak from the solvent.

Table 2. Vicinal ^{1}H−^{1}H Coupling Constants of 2MPD[a]

solvent or method	$^3J_T'^{HH}$	$^3J_G'^{HH}$	$^3J_G''^{HH}$	$^3J_G'''^{HH}$	$^3J_G^{HH}$
NMR Experiment[b]					
cyclohexane-d_{12}	11.81	2.74	2.38	4.19	3.10
chloroform-d	12.00	2.80	2.34	4.05	3.06
dimethyl-d_6 sulfoxide	11.75	2.78	2.34	3.92	3.01
methanol-d_4	11.96	2.77	2.21	3.95	2.98
deuterium oxide	12.24	2.93	2.17	4.07	3.06
MO Calculation[c]					
B3LYP/6-311+G(2d, p)	10.17	2.56	2.42	4.04	3.01
HF/6-311+G(2d, p)	12.71	4.04	3.85	5.97	4.62

[a] In Hz. For definitions of the coupling constants, see Figure 4. $^3J_T^{HH} = {}^3J_T'^{HH}$ and $^3J_G^{HH} = (^3J_G'^{HH} + {}^3J_G''^{HH} + {}^3J_G'''^{HH})/3$. [b] The ^3J values observed at 15, 25, 35, 45, and 55 °C were averaged. [c] Calculated with the Gaussian03W program.[17]

tri-MPDA, trans fractions for the NHC−C bond, ranging from 0.35 to 0.45, agree with those (0.35−0.48) of di-MPDA, and p_t^{CC}'s (0.41−0.61) for the C−CN(CH_3) bond are close to those (0.43−0.59) of tetra-MPDA.

3.2. ^{13}C NMR. Figure 2c shows observed and calculated ^{13}C NMR spectra of the methyl carbon of di-MPDA. The triplet is due to the vicinal coupling ($^3J_{CH}$) between the methyl carbon and methylene protons, A and A′. The $^3J_{CH}$ values for the five solutions are listed in Table 1. Shown in Figures 6 and 7 are ^{13}C NMR spectra of methyl carbons of tri-MPDA and tetra-MPDA, respectively; the vicinal coupling constants are given in the Supporting Information.

For di-MPDA and carbon A of tri-MPDA (Figure 1), the observed $^3J_{CH}$ value is expressed as

$$^3J_{CH} = {}^3J_G^{CH}\, p_t^{CN} + \frac{{}^3J_T^{CH} + {}^3J_G^{CH}}{2} p_g^{CN} \tag{4}$$

where $^3J_G^{CH}$ and $^3J_T^{CH}$ are defined in Figure 3, and p_t^{CN}

Table 3. Bond Conformations of di-MPDA and PTMI

method	medium	permittivity	temp, °C	p_t^{CC}	p_t^{CN}
		di-MPDA			
MO[a]	gas phase	1.00	15	0.24	0.74
			25	0.25	0.73
			35	0.25	0.72
			45	0.26	0.71
			55	0.27	0.71
NMR	cyclohexane-d_{12}	2.02	15	0.36	0.89
			25	0.36	0.86
			35	0.36	0.84
			45	0.35	0.83
			55	0.35	0.82
	chloroform-d	4.81	15	0.35	0.88
			25	0.35	0.86
			35	0.35	0.84
			45	0.35	0.81
			55	0.36	0.79
	dimethyl-d_6 sulfoxide	46.7	15	0.35	0.91
			25	0.35	0.88
			35	0.35	0.85
			45	0.35	0.83
			55	0.35	0.80
	methanol-d_4	32.7	15	0.48	0.70
			25	0.48	0.67
			35	0.47	0.65
			45	0.46	0.62
			55	0.45	0.61
	deuterium oxide	78.5	15	0.45	0.81
			25	0.46	0.77
			35	0.46	0.75
			45	0.46	0.72
			55	0.46	0.66
		PTMI			
IRIS[b]			15	0.28	0.78
			25	0.29	0.77
			35	0.29	0.76
			45	0.30	0.75
			55	0.30	0.75

[a] Calculated from the conformer free energies at 25 °C (Table 5). [b] Calculated with eq 21 from the conformational energies (Table 6).

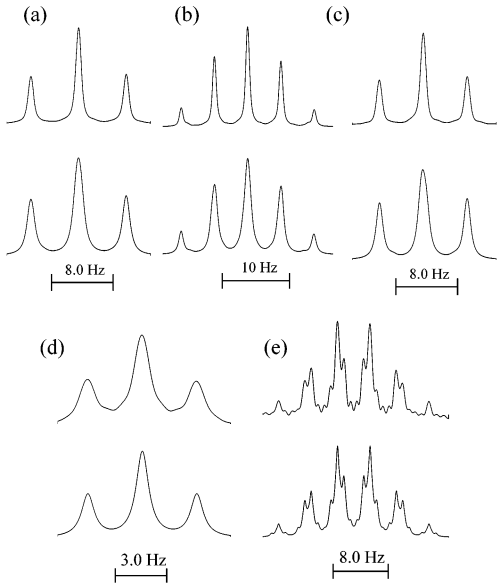

Figure 6. ^{1}H NMR spectra of methylene protons, (a) B, (b) C, and (c) D; ^{13}C NMR spectra of methyl carbons, (d) A and (e) E, of tri-MPDA in cyclohexane-d_{12} at 25 °C. The observed and calculated spectra are shown above and below, respectively. For designations of the atoms, see Figure 1.

and p_g^{CN} are trans and gauche fractions of the C−N bond, respectively. The definition dictates that

$$p_t^{CN} + p_g^{CN} = 1 \tag{5}$$

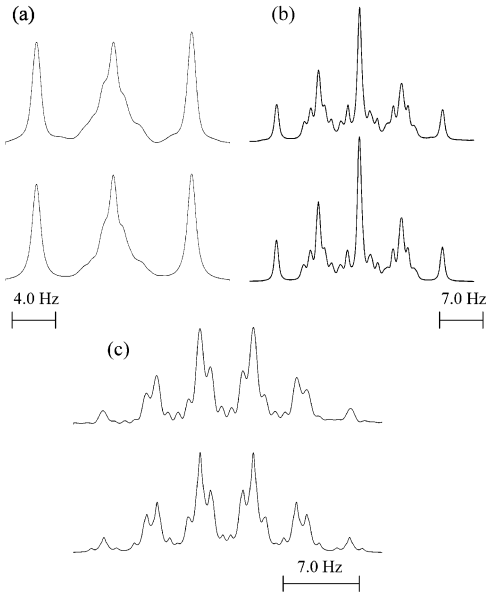

Figure 7. (a) ^{1}H NMR spectra of methylene protons, (a) B and (b) C; (c) ^{13}C NMR spectra of methyl carbons of tetra-MPDA dissolved in chloroform-d at 25 °C. The observed and calculated spectra are shown above and below, respectively. For designations of the atoms, see Figure 1.

Table 4. Bond Conformations of tri-MPDA, tetra-MPDA, and PMTMI at 25 °C

		p_t			p_{C_1} or p_t[a]
	method and medium	NH−C	NHC−C	C−CN(CH$_3$)	C−N(CH$_3$)
		tri-MPDA			
MO[b]	gas phase	0.76	0.26	0.26	0.99
NMR	cyclohexane-d_{12}	0.89	0.35	0.41	
	chloroform-d	0.88	0.44	0.47	
	dimethyl-d_6 sulfoxide	0.74	0.40	0.45	
	methanol-d_4	0.82	0.45	0.61	
	deuterium oxide	0.76	0.41	0.61	
		tetra-MPDA			
MO[b]	gas phase			0.38	0.98
NMR	cyclohexane-d_{12}			0.43	
	chloroform-d			0.55	
	dimethyl-d_6 sulfoxide			0.48	
	methanol-d_4			0.59	
	deuterium oxide			0.58	
		PMTMI			
IRIS[c]				0.40	0.65

[a] p_{C_1} for tri-MPDA and tetra-MPDA and p_t for PMTMI. [b] Calculated from the conformer free energies at the MP2/6-311++G(3df, 3pd)//HF/6-31G(d) level (Supporting Information). [c] Calculated from the conformational energies (Table 6).

The $^3J_T^{CH}$ values[1] determined from 2-methylpiperazine-5-^{13}C have been used here. The $^3J_G^{CH}$ values were obtained from *N,N,N′,N′*-tetramethylethylenediamine (tetra-MEDA) on the assumption that $p_{C_1} \approx 1$ and $p_{C_s} \approx 0$.[1] The ^{13}C− ^{1}H vicinal coupling constants around C−N(CH$_3$) bonds of tri-MPDA and tetra-MPDA (Supporting Information), designated as $^3J'_{CH}$, are almost equal to those of *N,N,N′*-trimethylethylenediamine (tri-MEDA) and tetra-MEDA.[1] These facts indicate the validity of the above assumption. For the details, see section 3.5 of ref 1. The bond conformations of di-MPDA and tri-MPDA, derived from eqs 4 and 5, are listed in Tables 3 and 4, respectively. For all the solutions of di-MPDA, the p_t^{CN} value decreases with an increase in temperature.

In Tables 3 and 4, bond conformations of the three model compounds, calculated with eqs 1 and 2 of ref 1

Table 5. Conformer Free Energies (ΔG_k's, kcal mol^{-1}) of di-MPDA, Evaluated from Ab Initio MO Calculations

		racemo (*ld*)		*meso* (*ll*)				*racemo* (*ld*)		*meso* (*ll*)	
k	conformation	statistical weight[a]	ΔG_k[b]	statistical weight[a]	ΔG_k[b]	k	conformation	statistical weight[a]	ΔG_k[b]	statistical weight[a]	ΔG_k[b]
1	t t t t	1	0.00	1	0.21	42	$g^+ g^+ g^+ g^-$	0		$\gamma^2\sigma^2\nu\omega$	3.84
2	t t t g^+	γ	1.14	δ	0.63	43	$g^+ g^+ g^-$ t	$\gamma\sigma^2\psi'$	2.82	$\gamma\sigma^2\psi''$	0.73
3	t t t g^-	δ	0.80	γ	1.12	44	$g^+ g^+ g^- g^+$	0		0	
4	t t g^+ t	$\sigma\eta$	0.15	$\sigma\nu$	0.27	45	$g^+ g^+ g^- g^-$	$\delta\gamma\sigma^2\psi''$	1.22	$\gamma^2\sigma^2\psi'$	4.00
5	t t $g^+ g^+$	$\gamma\sigma\nu$	1.24	$\delta\sigma\eta$	0.51	46	$g^+ g^-$ t t	$\gamma\sigma\omega$	2.78	$\gamma\sigma\omega$	3.14
6	t t $g^+ g^-$	$\delta\sigma\omega$	2.61	$\gamma\sigma\omega$	3.14	47	$g^+ g^-$ t g^+	$\gamma^2\sigma\omega$	4.34	$\delta\gamma\sigma\omega$	3.71
7	t t g^- t	$\sigma\nu$	0.38	$\sigma\eta$	−0.11	48	$g^+ g^-$ t g^-	$\delta\gamma\sigma\omega$	3.74	$\gamma^2\sigma\omega$	4.00
8	t t $g^- g^+$	$\gamma\sigma\omega$	2.78	$\delta\sigma\omega$	2.78	49	$g^+ g^- g^+$ t	0		0	
9	t t $g^- g^-$	$\delta\sigma\eta$	0.27	$\gamma\sigma\nu$	1.04	50	$g^+ g^- g^+ g^+$	0		0	
10	t g^+ t t	$\sigma\eta$	0.15	$\sigma\eta$	−0.11	51	$g^+ g^- g^+ g^-$	0		0	
11	t g^+ t g^+	$\gamma\sigma\eta$	1.11	$\delta\sigma\eta$	0.73	52	$g^+ g^- g^-$ t	$\gamma\sigma^2\nu\omega$	2.87	$\gamma\sigma^2\eta\omega$	2.34
12	t g^+ t g^-	$\delta\sigma\eta$	0.40	$\gamma\sigma\eta$	1.18	53	$g^+ g^- g^- g^+$	$\gamma^2\sigma^2\omega^2$	6.40	$\delta\gamma\sigma^2\omega^2$	5.65
13	t $g^+ g^+$ t	$\sigma^2\eta^2$	−0.19	$\sigma^2\eta\nu$	−0.38	54	$g^+ g^- g^- g^-$	$\delta\gamma\sigma^2\eta\omega$	2.90	$\gamma^2\sigma^2\nu\omega$	3.84
14	t $g^+ g^+ g^+$	$\gamma\sigma^2\eta\nu$	0.48	$\delta\sigma^2\eta^2$	0.13	55	g^- t t t	δ	0.80	δ	0.63
15	t $g^+ g^+ g^-$	0		$\gamma\sigma^2\eta\omega$	2.34	56	g^- t t g^+	$\delta\gamma$	1.71	δ^2	1.41
16	t $g^+ g^-$ t	$\sigma^2\psi''$	−0.94	$\sigma^2\psi$	1.82	57	g^- t t g^-	δ^2	1.27	$\delta\gamma$	1.73
17	t $g^+ g^- g^+$	0		0		58	g^- t g^+ t	$\delta\sigma\eta$	0.40	$\delta\sigma\nu$	1.12
18	t $g^+ g^- g^-$	0		$\gamma\sigma^2\psi''$	0.73	59	g^- t $g^+ g^+$	$\delta\gamma\sigma\nu$	1.74	$\delta^2\sigma\eta$	0.79
19	t g^- t t	$\sigma\nu$	0.38	$\sigma\nu$	0.27	60	g^- t $g^+ g^-$	$\delta^2\sigma\omega$	3.61	$\delta\gamma\sigma\omega$	3.71
20	t g^- t g^+	$\gamma\sigma\nu$	1.42	$\delta\sigma\nu$	1.12	61	g^- t g^- t	$\delta\sigma\nu$	1.01	$\delta\sigma\eta$	0.73
21	t g^- t g^-	$\delta\sigma\nu$	1.01	$\gamma\sigma\nu$	1.40	62	g^- t $g^- g^+$	$\delta\gamma\sigma\omega$	3.74	$\delta^2\sigma\omega$	3.33
22	t $g^- g^+$ t	$\sigma^2\psi''$	−0.94	$\sigma^2\psi'$	1.62	63	g^- t $g^- g^-$	$\delta^2\sigma\eta$	1.09	$\delta\gamma\sigma\nu$	1.89
23	t $g^- g^+ g^+$	$\gamma\sigma^2\psi'$	2.82	$\delta\sigma^2\psi''$	−0.53	64	$g^- g^+$ t t	$\delta\sigma\omega$	2.61	$\delta\sigma\omega$	2.78
24	t $g^- g^+ g^-$	0		0		65	$g^- g^+$ t g^+	$\delta\gamma\sigma\omega$	3.44	$\delta^2\sigma\omega$	3.32
25	t $g^- g^-$ t	$\sigma^2\nu^2$	0.51	$\sigma^2\eta\nu$	−0.38	66	$g^- g^+$ t g^-	$\delta^2\sigma\omega$	3.61	$\delta\gamma\sigma\eta$	3.93
26	t $g^- g^- g^+$	$\gamma\sigma^2\nu\omega$	2.87	$\delta\sigma^2\nu\omega$	2.05	67	$g^- g^+ g^+$ t	0		$\delta\sigma^2\nu\omega$	2.05
27	t $g^- g^- g^-$	$\delta\sigma^2\eta\nu$	0.11	$\gamma\sigma^2\nu^2$	1.36	68	$g^- g^+ g^+ g^+$	0		0	
28	g^+ t t t	γ	1.14	γ	1.12	69	$g^- g^+ g^+ g^-$	$\delta^2\sigma^2\omega^2$	5.29	$\delta\gamma\sigma^2\omega^2$	5.65
29	g^+ t t g^+	γ^2	2.22	$\delta\gamma$	1.73	70	$g^- g^+ g^-$ t	0		0	
30	g^+ t t g^-	$\delta\gamma$	1.71	γ^2	2.22	71	$g^- g^+ g^- g^+$	0		0	
31	g^+ t g^+ t	$\gamma\sigma\eta$	1.11	$\gamma\sigma\nu$	1.40	72	$g^- g^+ g^- g^-$	0		0	
32	g^+ t $g^+ g^+$	$\gamma^2\sigma\nu$	2.27	$\delta\gamma\sigma\eta$	1.44	73	$g^- g^-$ t t	$\delta\sigma\eta$	0.27	$\delta\sigma\eta$	0.51
33	g^+ t $g^+ g^-$	$\delta\gamma\sigma\omega$	3.44	$\gamma^2\sigma\omega$	4.00	74	$g^- g^-$ t g^+	$\delta\gamma\sigma\eta$	1.54	$\delta^2\sigma\eta$	0.79
34	g^+ t g^- t	$\gamma\sigma\nu$	1.42	$\gamma\sigma\eta$	1.18	75	$g^- g^-$ t g^-	$\delta^2\sigma\eta$	1.09	$\delta\gamma\sigma\eta$	1.44
35	g^+ t $g^- g^+$	$\gamma^2\sigma\omega$	4.34	$\delta\gamma\sigma\omega$	3.93	76	$g^- g^- g^+$ t	0		$\delta\sigma^2\psi''$	−0.53
36	g^+ t $g^- g^-$	$\delta\gamma\sigma\eta$	1.54	$\gamma^2\sigma\nu$	2.36	77	$g^- g^- g^+ g^+$	$\delta\gamma\sigma^2\psi''$	1.22	$\delta^2\sigma^2\psi$	3.15
37	$g^+ g^+$ t t	$\gamma\sigma\nu$	1.24	$\gamma\sigma\nu$	1.04	78	$g^- g^- g^+ g^-$	0		0	
38	$g^+ g^+$ t g^+	$\gamma^2\sigma\nu$	2.27	$\delta\gamma\sigma\nu$	1.89	79	$g^- g^- g^-$ t	$\delta\sigma^2\eta\nu$	0.11	$\delta\sigma^2\eta^2$	0.13
39	$g^+ g^+$ t g^-	$\delta\gamma\sigma\nu$	1.74	$\gamma^2\sigma\nu$	2.36	80	$g^- g^- g^- g^+$	$\delta\gamma\sigma^2\eta\omega$	2.91	0	
40	$g^+ g^+ g^+$ t	$\gamma\sigma^2\eta\nu$	0.48	$\gamma\sigma^2\nu^2$	1.36	81	$g^- g^- g^- g^-$	$\delta^2\sigma^2\eta^2$	0.45	$\delta\gamma\sigma^2\eta\nu$	1.00
41	$g^+ g^+ g^+ g^+$	$\gamma^2\sigma^2\nu^2$	2.24	$\delta\gamma\sigma^2\eta\nu$	1.00						

[a] For interactions corresponding to the statistical weights, see Figures 3 and 8. [b] Relative to the G_k value of the *racemo* all-trans conformation. The blank indicates that the geometrical optimization did not detect the potential minimum; thus, the conformer is considered to be absent.

from the ab initio MO calculations (Table 5 and Supporting Information), are compared with the NMR observations. On the ground of fairly good agreement between theory and experiment, we proceeded to the conformational analysis of PTMI and PMTMI using the MO energies.

3.3. Statistical Weight Matrices and Conformational Energies of di-MPDA. As described in the Introduction, statistical weight matrices of di-MPDA and PTMI include first-order to fourth-order interactions. In the three-state (t, g^+, and g^-) scheme, the statistical weight matrices (U_2 and U_3) of bonds 2 and 3 are given as 3×3 and 3×9 ones, respectively. The U_5 matrix, including the above-mentioned fourth-order interactions, is 27×27. For the matrix multiplication, the U_4 matrix must be 9×27. From careful investigation of the molecular models, the $U_2 - U_4$ matrices were formulated for each configuration as shown in Figure 12 (Appendix). The stereochemical configurations are based on the pseudoasymmetry (see Figure 1).[1−3,29−31] Intramolecular interactions defined for di-MPDA and PTMI are illustrated in Figures 3 and 8. Fourth-order ψ, ψ', and ψ'' interactions, representing the lone pair ··· lone pair, N−H···H−N, and N−H···lone pair contacts respectively, are included in the U_5 matrices (Figure 13 in Appendix). The U_5 matrices for the *dd* and *dl* forms can be, respectively, derived from those of the *ll* and *ld* ones according to

$$U_5^{dd} = Q_{27} U_5^{ll} Q_{27} \tag{6}$$

and

$$U_5^{dl} = Q_{27} U_5^{ld} Q_{27} \tag{7}$$

where the superscript represents the configuration and Q_{27} is given by

$$Q_{27} = Q_3 \otimes Q_3 \otimes Q_3 \tag{8}$$

Here, $\otimes$ stands for direct product, and Q_3 is defined as

$$Q_3 = \begin{pmatrix} 1 & 0 & 0 \\ 0 & 0 & 1 \\ 0 & 1 & 0 \end{pmatrix} \tag{9}$$

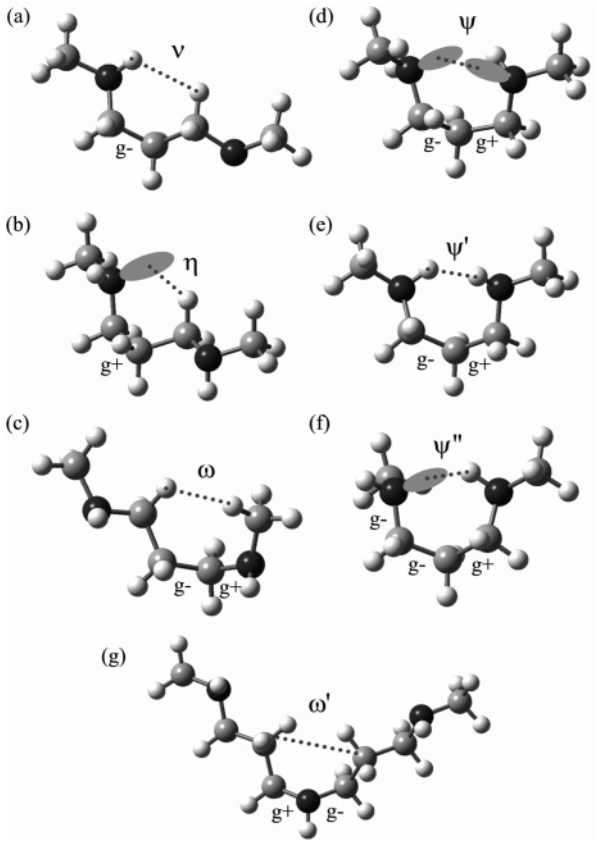

Figure 8. Second-order, third-order, and fourth-order intramolecular interactions defined for di-MPDA and PTMI. The trans conformations are not displayed.

The Q_{27} matrix satisfies the relation

$$Q_{27}Q_{27} = I_{27} \tag{10}$$

where I_{27} is the identity matrix of size 27.

From the U matrices, statistical weights of the individual conformers of di-MPDA can be obtained as shown in Table 5. The statistical weight is related to the corresponding conformational energy through the Boltzmann factor; for example, $\gamma = \exp(-E_\gamma/RT)$, where R is the gas constant, and T is the absolute temperature. The conformational energies, E_ξ's ($\xi = \gamma$, δ, σ, ν, η, ω, ψ, ψ', and ψ''), were determined by minimizing the following function

$$S(\mathbf{E}) = \frac{1}{K}\sum_{k}^{K}[\sum_{\xi}L(\xi)E_\xi - \Delta G_k]^2\exp(-\Delta G_k/RT) \tag{11}$$

where K is the number of conformers. The function $L(\xi)$ gives the number of conformational energy E_ξ included in the conformation. The Boltzmann factor $\exp(-\Delta G_k/RT)$ was introduced so as to weight low-energy conformers. The temperature T was set to 298.15 K. The initial E_ξ values were estimated from ΔG_k's of the representative conformers, and, consequently, a single set of E_ξ's were determined (Table 6).

The first-order interaction energies, E_γ, E_δ, and E_σ, were obtained as 1.16 (1.06), 0.53 (0.54), and −0.06 (−0.09) kcal mol^{-1}, respectively. Here, the values in the parentheses represent the corresponding energies of *N*, *N*′-dimethylethylenediamine (di-MEDA) and PEI.[1] The pentane-effect-like ω interaction is a repulsion (E_ω = 1.78 kcal mol^{-1}) comparable to that (∼2 kcal mol^{-1}) of *n*-alkanes.[2,32] The ν interaction appears to be noneffective (E_ν = 0.06 kcal mol^{-1}). Figure 8b shows the η interaction to be a C−H···N hydrogen bond, which seems very weak (E_η = −0.15 kcal mol^{-1}). It should be noted that the ν and η interactions of di-MPDA are different from those of di-MEDA.[1] The lone pair···lone pair and N−H···H−N interactions are repulsive: E_ψ = 1.89 kcal mol^{-1} and $E_{\psi'}$ = 1.74 kcal mol^{-1}. The ψ'' interaction is an N−H···N hydrogen bond ($E_{\psi''}$ = −0.83 kcal mol^{-1}, Figure 8f), being intermediate in strength between those of di-MEDA (−1.54 and −0.58 kcal mol^{-1}).[1] Two kinds of intramolecular hydrogen bonds were found in di-MPDA: a weak C−H···N and a moderate N−H···N attractions.

Table 6. Conformational Energies (kcal mol^{-1}) of di-MPDA (PTMI) and tetra-MPDA (PMTMI), Derived from Ab Initio MO Calculations[a]

	di-MPDA (PTMI)	tetra-MPDA (PMTMI)	di-MEDA[b] (PEI)
	First-Order Interaction		
E_γ	1.16	1.41	1.06
E_δ	0.53		0.54
E_σ	−0.06	−0.11	−0.09
	Second- and Third-Order Interactions		
E_ν	0.06		
E_η	−0.15	−0.40	
E_ω	1.78	2.11	
$E_{\omega'}$[c]	1.22	0.59	
	Fourth-Order Interaction		
E_ψ	1.89		
$E_{\psi'}$	1.74		
$E_{\psi''}$	−0.83		

[a] At the MP2/6-311++G(3df, 3pd)//HF/6-31G(d) level. For definitions of the interactions, see Figures 3, 8, and 9. [b] For the sake of comparison, first-order interaction energies of di-MEDA (PEI) are shown.[1] [c] Evaluated from free energies of tttg$^+$g$^-$ttt, tttg$^+$tttt, and ttttg$^-$ttt conformers of dimers (PTMI, $CH_3NH(CH_2CH_2CH_2NH)_2CH_3$; PMTMI, $(CH_3)_2N(CH_2CH_2CH_2NCH_3)_2CH_3$) according to $E_{\omega'} = \Delta G_{\text{tttg}^+\text{g}^-\text{ttt}} - \Delta G_{\text{tttg}^+\text{tttt}} - \Delta G_{\text{ttttg}^-\text{ttt}}$.

3.4. Statistical Weight Matrices of PTMI. Statistical weight matrices for bonds a, b, and c are satisfactorily expressed with up to third-order interactions. For the matrix operation, however, the U_a, U_b, and U_c matrices must be 27 × 27, thus being composed of three identical 9 × 27 block matrices (Figure 14 in Appendix). The U_d^α matrix is equal to U_5^α (α = *ll*, *dd*, *ld*, or *dl*). Statistical weight matrices of the *dd* and *dl* forms can be derived from

$$U_\beta^{dd} = Q_{27}U_\beta^{ll}Q_{27} \tag{12}$$

and

$$U_\beta^{dl} = Q_{27}U_\beta^{ld}Q_{27} \tag{13}$$

where β = a, b, c, and d. In U_a's, a new weight ω', representing a pentane-effect-like C−H···H−C repulsion (see Figure 8g), is introduced. The $E_{\omega'}$ value (1.22 kcal mol^{-1}) was calculated from a dimer $CH_3NH(CH_2CH_2CH_2NH)_2CH_3$.

3.5. IRIS Scheme with up to Fourth-Order Interactions: Diad Probability and Bond Conformation. The *meso*-diad probability at the *i*th repeating unit, $P_{m;i}$, can be calculated from

$$P_{m;i} = Z^{-1}J^*(\prod_{h=1}^{i-1}W_h)W_i^m(\prod_{h=i+1}^{x}W_h)J \tag{14}$$

where Z is the partition function of the whole chain including all possible stereosequences,

$$Z = J^*(\prod_{i=1}^{x} W_i)J \tag{15}$$

W_i is a combined statistical weight matrix of the ith unit,

$$W_i = \begin{pmatrix} V_i^{ll} & V_i^{ld} \\ V_i^{dl} & V_i^{dd} \end{pmatrix} \tag{16}$$

W_i^m is the matrix for the *meso* form

$$W_i^m = \begin{pmatrix} V_i^{ll} & 0 \\ 0 & V_i^{dd} \end{pmatrix} \tag{17}$$

x is the degree of polymerization, $J^* = [\,1\ 0\ 0\ ...]$, and J is the column matrix whose elements are unity. The sizes of J^* and J depend on those of the following and preceding matrices, respectively. Here, the V_i^α matrix ($\alpha = ll$, dd, ld, or dl) is defined as

$$V_i^\alpha = \begin{cases} U_2^\alpha\, U_3^\alpha\, U_4^\alpha\, U_5^\alpha & \text{for } i = 1 \\ U_\mathrm{a}^\alpha\, U_\mathrm{b}^\alpha\, U_\mathrm{c}^\alpha\, U_\mathrm{d}^\alpha & \text{for } i \geq 2 \end{cases} \tag{18}$$

The P_m value of the whole chain is given as the average of $P_{m;i}$'s:

$$P_m = x^{-1}\sum_{i=1}^{x} P_{m;i} \tag{19}$$

The *racemo*-diad probability P_r is obtained from

$$P_r = 1 - P_m \tag{20}$$

Bond conformations averaged over all the stereosequences can be calculated as follows. For example, the trans fraction ($p_{\mathrm{t;a};i}$) in bond a of the ith repeating unit is derived from

$$p_{\mathrm{t;a};i} = Z^{-1}J^*(\prod_{h=1}^{i-1} W_h)W_{\mathrm{t;a}}(\prod_{h=i+1}^{x} W_h)J \tag{21}$$

where

$$W_{\mathrm{t;a}} = \begin{pmatrix} V_{\mathrm{t;a}}^{ll} & V_{\mathrm{t;a}}^{ld} \\ V_{\mathrm{t;a}}^{dl} & V_{\mathrm{t;a}}^{dd} \end{pmatrix} \tag{22}$$

with $V_{\mathrm{t;a}}^\alpha$ being

$$V_{\mathrm{t;a}}^\alpha = U_{\mathrm{t;a}}^\alpha\, U_\mathrm{b}^\alpha\, U_\mathrm{c}^\alpha\, U_\mathrm{d}^\alpha \tag{23}$$

In $U_{\mathrm{t;a}}^\alpha$, the columns of the trans state are equal to those of U_a^α, and the other elements are filled with zero. In the similar manner, trans and gauche fractions can be calculated for each bond.[33]

3.6. IRIS Scheme with up to Fourth-Order Interactions: Mean-Square End-to-End Distance. The mean-square end-to-end distance $\langle r^2\rangle$ is given by

$$\langle r^2\rangle = 2z^{-1}J^*G_1G_2G_3G_4G_5...G_nJ^{**} \tag{24}$$

where $J^{**} = [0...01...1]^T$,[34] and z is the partition function of the polymeric chain, being calculated from

$$z = J^*U_2U_3U_4U_5...U_{n-1}J \tag{25}$$

with n being the number of bonds. The G_j matrix of the jth bond is defined as

$$G_j = \begin{pmatrix} U_j & (U_j \otimes \bar{l}_j^T)||T||_j & (l_j^2/2)U_j \\ 0 & (U_j \otimes I_3)||T||_j & U_j \otimes \bar{l}_j \\ 0 & 0 & U_j \end{pmatrix} \tag{26}$$

where l_j is the bond length, I_3 is the identity matrix of size 3, and $\bar{l}_j$ is given by

$$\bar{l}_j = l_j\begin{pmatrix} 1 \\ 0 \\ 0 \end{pmatrix} \tag{27}$$

The $||T||_j$ matrix is defined as

$$||T||_j = \begin{cases} \tau_j & j = 1 \text{ and } 2 \\ I_3 \otimes \tau_j & j = 3 \\ I_3 \otimes I_3 \otimes \tau_j & j \geq 4 \end{cases} \tag{28}$$

where in the three-state scheme, τ_j is given by

$$\tau_j = \begin{pmatrix} T_{\mathrm{t};j} & 0 & 0 \\ 0 & T_{g^+;j} & 0 \\ 0 & 0 & T_{\mathrm{g}^-;j} \end{pmatrix} \tag{29}$$

The T matrix transforms a vector from the jth to ($j - 1$)th frame of reference. For example, $T_{\mathrm{t};j}$ is expressed as

$$T_{\mathrm{t};j} = \begin{pmatrix} \cos\theta_{\mathrm{t};j} & \sin\theta_{\mathrm{t};j} & 0 \\ \sin\theta_{\mathrm{t};j}\cos\phi_{\mathrm{t};j} & -\cos\theta_{\mathrm{t};j}\cos\phi_{\mathrm{t};j} & \sin\phi_{\mathrm{t};j} \\ \sin\theta_{\mathrm{t};j}\sin\phi_{\mathrm{t};j} & -\cos\theta_{\mathrm{t};j}\sin\phi_{\mathrm{t};j} & -\cos\phi_{\mathrm{t};j} \end{pmatrix} \tag{30}$$

where $\theta_{\mathrm{t};j}$ is the supplement of the bond angle, and $\phi_{\mathrm{t};j}$ is the dihedral angle for the trans state of the jth bond. The sizes of the block matrices of G_j are

$$\begin{pmatrix} s \times t & s \times 3t & s \times t \\ 3s \times t & 3s \times 3t & 3s \times t \\ s \times t & s \times 3t & s \times t \end{pmatrix} \tag{31}$$

where (s, t) corresponds to the size of U_j.

The configurational sequence of the PTMI chain can be chosen according to the algorithm of the Monte Carlo chain. The details are described in section 3.9 of ref 1. The H_i^α matrix of the ith unit is defined for each configuration as

$$H_i^\alpha = \begin{cases} G_2^\alpha\, G_3^\alpha\, G_4^\alpha\, G_5^\alpha & \text{for } i = 1 \\ G_\mathrm{a}^\alpha\, G_b^\alpha\, G_\mathrm{c}^\alpha\, G_\mathrm{d}^\alpha & \text{for } i \geq 2 \end{cases} \tag{32}$$

The mean-square end-to-end distance, $\langle r^2\rangle_m$, of the mth chain in the system can be calculated from[34]

$$\langle r^2\rangle_m = 2{z_m}^{-1}J^*G_1(\prod_{i=1}^{x} H_i^\alpha)G_nJ^{**} \tag{33}$$

Here, z_m is the partition function of the mth chain, and the H_i^α matrices are arranged as determined by the

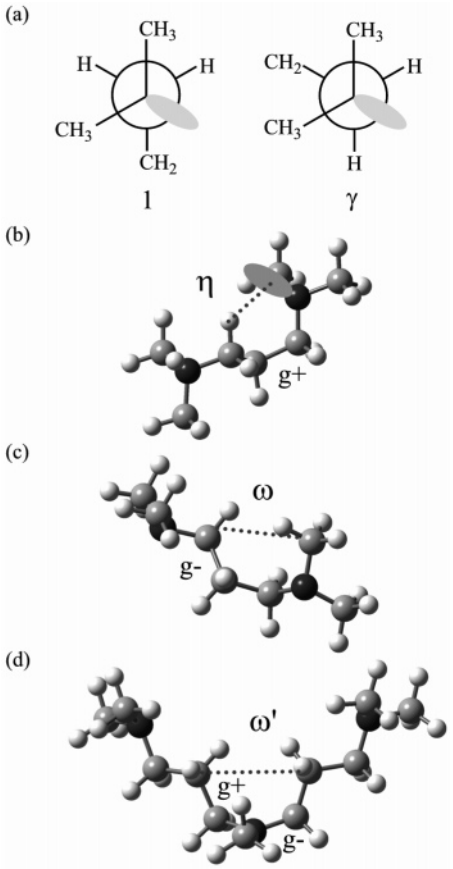

Figure 9. First-order, second-order, and third-order intramolecular interactions defined for tetra-MPDA and PMTMI. The first-order interaction (σ) around the C−C bond is equivalent to that of di-MPDA and PTMI (Figure 3b), The trans conformations are not displayed.

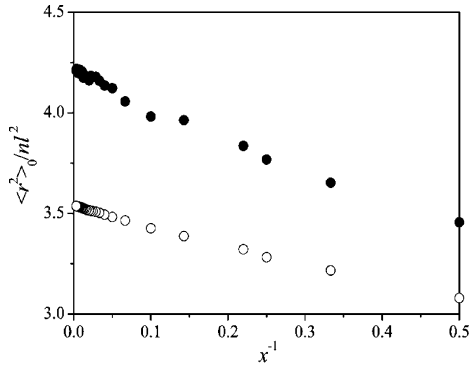

Figure 10. Characteristic ratios of PTMI (open circle) and PMTMI (filled circle) ensembles of $n_c = 512$ as a function of the reciprocal degree of polymerization.

Monte Carlo method. The ensemble average of $\langle r^2\rangle_m$'s is given by

$$\langle r^2\rangle = \frac{\sum_{m=1}^{n_c}\langle r^2\rangle_m z_m}{\sum_{m=1}^{n_c} z_m} \tag{34}$$

where n_c is the total number of chains included in the system. When the sampling number ($x \times n_c$) is large enough, the $\langle r^2\rangle$ value is satisfactorily approximated by[35]

$$\langle r^2\rangle = \frac{\sum_{m=1}^{n_c}\langle r^2\rangle_m}{n_c} \tag{35}$$

The characteristic ratio $\langle r^2\rangle/nl^2$ can be obtained from the $\langle r^2\rangle$ value, the number of bonds, and the bond lengths (l's). If bond dipole moments are substituted for the bond lengths in eqs 26 and 27, then eqs 34 and 35 yield the mean-square dipole moment, $\langle \mu^2\rangle$.

3.7. Statistical Weight Matrices and Conformational Energies of tetra-MPDA and PMTMI. For tetra-MPDA and PMTMI, severe steric repulsions between bulky $N(CH_3)$ groups allow us to take no account of fourth-order interactions between the nitrogen sites and formulate the statistical weight matrices in 9 × 9 forms. First-order (γ and σ) and second- and third-order (η, ω, and ω') interactions of tetra-MPDA and PMTMI are analogous to those of di-MPDA (see Figures 3, 8, and 9). For the U matrices, see Figures 15 and 16

Table 7. Geometrical Parameters Used in IRIS Calculations for PTMI and PMTMI[a]

			dihedral angle, deg					
			PTMI			PMTMI		
configuration		bond	t	g^+	g^-	t	g^+	g^-
meso	*ll*	a	0.0	113.0	−103.8	−15.7	112.3	−112.6
		b	0.0	118.0	−112.3	6.4	121.6	−73.8
		c	0.0	112.3	−118.0	−6.4	73.8	−121.6
		d	0.0	103.8	−113.0	15.7	112.6	−112.3
	dd	a	0.0	103.8	−113.0	15.7	112.6	−112.3
		b	0.0	112.3	−118.0	−6.4	73.8	−121.6
		c	0.0	118.0	−112.3	6.4	121.6	−73.8
		d	0.0	113.0	−103.8	−15.7	112.3	−112.6
racemo	*ld*	a	0.0	113.5	−102.7	−13.4	114.8	−110.2
		b	0.0	116.1	−114.2	10.6	123.5	−74.8
		c	0.0	116.1	−114.2	10.6	123.5	−74.8
		d	0.0	113.5	−102.7	−13.4	114.8	−110.2
	dl	a	0.0	102.7	−113.5	13.4	110.2	−114.8
		b	0.0	114.2	−116.1	−10.6	74.8	−123.5
		c	0.0	114.2	−116.1	−10.6	74.8	−123.5
		d	0.0	102.7	−113.5	13.4	110.2	−114.8

[a] On the basis of the geometrical optimization for di-MPDA and tetra-MPDA at the HF/6-31G(d) level. Bond lengths and bond angles for PTMI (PMTMI) are as follows: l_{CN} = 1.45 (1.45) Å, l_{CC} = 1.52 (1.53) Å, ∠CNC = 113.8 (111.5)° ∠NCC = 111.0 (113.6)°, and ∠CCC = 113.0 (111.2)°.

Table 8. First Derivatives of the Characteristic Ratio, *meso*-Diad Probability, and Bond Conformations of PTMI and PMTMI at 25 °C with Respect to Conformational Energies (E_ξ's)[a]

	$\partial X/\partial E_\xi$ (10^{-3} kcal^{-1} mol)							
	PTMI				PMTMI			
E_ξ	X: $\langle r^2\rangle_0/nl^2$	X: P_m	X: p_t^{CC}	X: p_t^{CN}	X: $\langle r^2\rangle_0/nl^2$	X: P_m	X: p_t^{CC}	X: p_t^{CN}
E_γ	−81	−28	−10	80	−230	−2.5	−20	35
E_δ	−370	−74	−30	180				
E_σ	3500	55	360	−50	2500	22	340	−10
E_ν	−1100	−34	20	10				
E_η	−1200	−44	30	10	2400	23	340	−20
E_ω	−9.5	−1.0	0.0	5.0	−51	−1.0	5.0	0.0
$E_{\omega'}$	18	−2.5	0.0	5.0	28	0.0	0.0	0.0
E_ψ	12	−1.5	0.0	0.0				
$E_{\psi'}$	14	−1.0	0.0	0.0				
$E_{\psi''}$	2900	70	160	−20				

[a] At the individual E_ξ values shown in Table 6. The other energies were set as in Table 6.

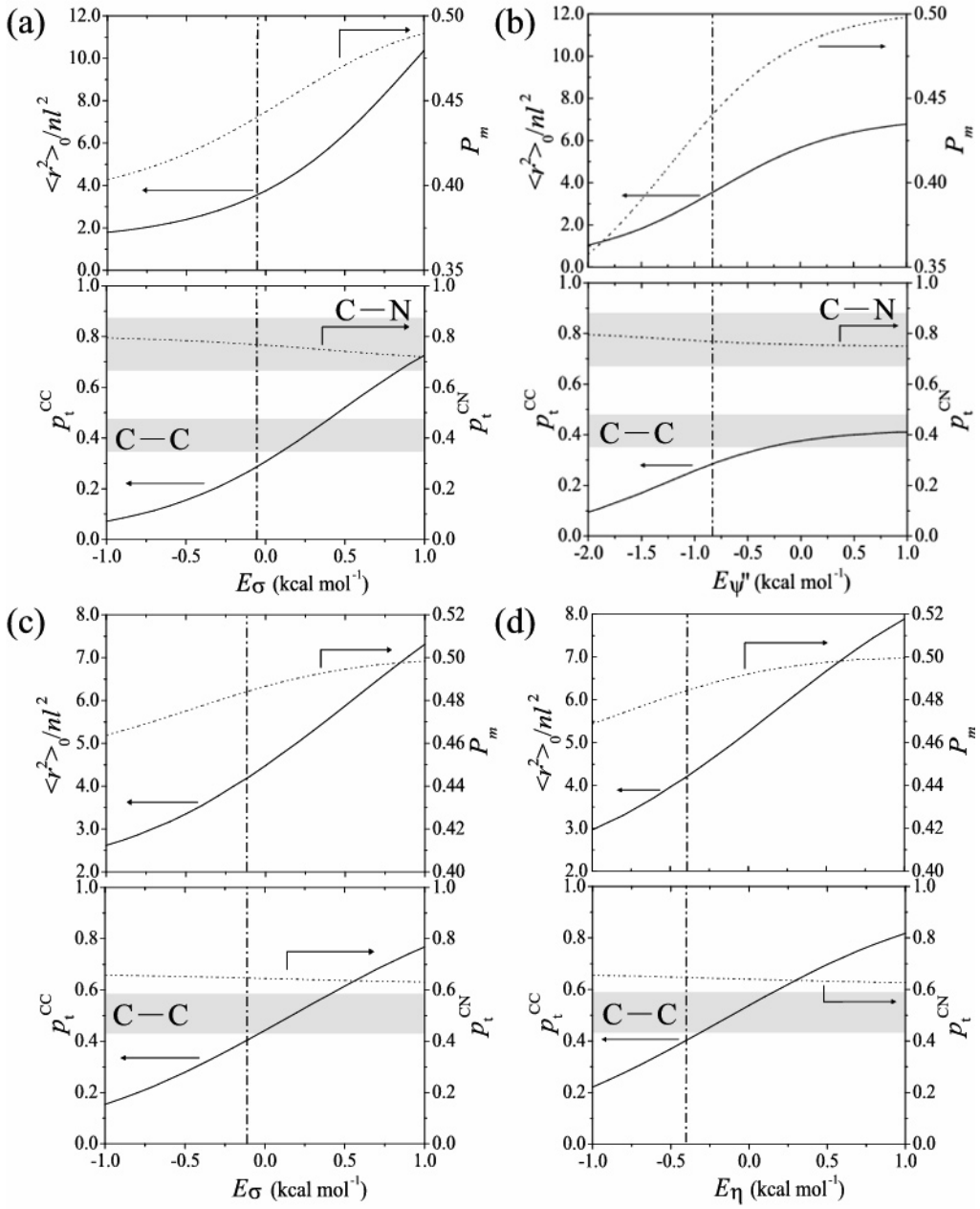

Figure 11. Characteristic ratio, *meso*-diad probability, and trans fractions of the C−C and C−N bonds as a function of (a) E_σ or (b) $E_{\psi''}$ (PTMI) and (c) E_σ or (d) E_η (PMTMI). The vertical dash−dotted line corresponds to the energy value shown in Table 6. The horizontal shaded regions represent the p_t^{CC} and p_t^{CN} ranges derived from the NMR experiments.

(Appendix). The IRIS scheme using 9 × 9 statistical weight matrices is partly described in ref 1 and may be analogized from sections 3.5 and 3.6 of this paper. The ΔG_k values and statistical weights of tetra-MPDA are given in the Supporting Information, and the conformational energies determined with eq 11 from the ΔG_k values are listed in Table 6.

The E_γ value is larger than that of di-MPDA because of the additional methyl group (cf. Figures 3a and 9a). The small negative E_σ value is close to those of di-MPDA and di-MEDA. As depicted in Figure 9, the η interaction corresponds to a C−H···N hydrogen bond ($E_\eta = -0.40$ kcal mol^{-1}).[36] The ω interaction was evaluated as $E_\omega =$ 2.11 kcal mol^{-1}. The ω' interaction, which is formed in, e.g., the g^-g^+ conformation for the C−N/N−C bonds linked with the *l* nitrogen site (Figure 9d), is comparatively weak ($E_{\omega'} = 0.59$ kcal mol^{-1}). On the other hand, in the g^+g^- conformation for the C−N/N−C bonds, no potential minimum was found; therefore, the sixth columns of U_a^{ll} and U_a^{ld} are filled with zero.

3.8. Characteristic Ratios, Diad Probabilities, and Bond Conformations of PTMI and PMTMI. The characteristic ratio, diad probability, and bond conformations of PTMI were calculated with geometrical parameters in Table 7 and conformational energies in Table 6. The $\langle r^2\rangle_0/nl^2$ values of the PTMI ensemble of $n_c = 512$ at 25 °C are plotted against the reciprocal degree (x^{-1}) of polymerization (Figure 10). The data form a smooth curve, which monotonically decreases with increasing x^{-1} and intersects with $x^{-1} = 0$ at $\langle r^2\rangle_0/nl^2 =$ 3.5. This value corresponds to the characteristic ratio for the infinite chain ($x \rightarrow \infty$). At 25 °C, the temperature coefficient, $10^3\, d \ln \langle r^2\rangle_0/dT$, is 2.6 K^{-1}, the *meso*-diad probability, P_m, is 0.44, and trans fractions in the C−C and C−N bonds are 0.29 and 0.77, respectively. The bond conformations at 15−55 °C are listed in Table 3.

(a)

$$U_2^{ll} = U_2^{ld} = \begin{array}{c} \\ t \\ g^+ \\ g^- \end{array} \begin{array}{c} \begin{array}{ccc} t & g^+ & g^- \end{array} \\ \begin{pmatrix} 1 & \gamma & \delta \\ 0 & 0 & 0 \\ 0 & 0 & 0 \end{pmatrix} \end{array}$$

(b)

$$U_2^{dd} = U_2^{dl} = \begin{array}{c} \\ t \\ g^+ \\ g^- \end{array} \begin{array}{c} \begin{array}{ccc} t & g^+ & g^- \end{array} \\ \begin{pmatrix} 1 & \delta & \gamma \\ 0 & 0 & 0 \\ 0 & 0 & 0 \end{pmatrix} \end{array}$$

(c)

$$U_3^{ll} = U_3^{dd} = U_3^{ld} = U_3^{dl} = \begin{array}{c} \\ t \\ g^+ \\ g^- \end{array} \begin{array}{c} \begin{array}{ccccccccc} t & g^+ & g^- & t & g^+ & g^- & t & g^+ & g^- \end{array} \\ \begin{pmatrix} 1 & \sigma & \sigma & 0 & 0 & 0 & 0 & 0 & 0 \\ 0 & 0 & 0 & 1 & \sigma & \sigma & 0 & 0 & 0 \\ 0 & 0 & 0 & 0 & 0 & 0 & 1 & \sigma & \sigma \end{pmatrix} \end{array}$$

(d)

$$U_4^{ll} = U_4^{ld} = \begin{array}{c} \\ t\ t \\ t\ g^+ \\ t\ g^- \\ g^+t \\ g^+g^+ \\ g^+g^- \\ g^-t \\ g^-g^+ \\ g^-g^- \end{array} \begin{array}{c} \begin{array}{ccccccccccccccccccccccccccc} t & g^+ & g^- & t & g^+ & g^- & t & g^+ & g^- & t & g^+ & g^- & t & g^+ & g^- & t & g^+ & g^- & t & g^+ & g^- & t & g^+ & g^- & t & g^+ & g^- \end{array} \\ \begin{pmatrix} 1 & \sigma & \sigma & 0 & 0 & 0 & 0 & 0 & 0 & 0 & 0 & 0 & 0 & 0 & 0 & 0 & 0 & 0 & 0 & 0 & 0 & 0 & 0 & 0 & 0 & 0 & 0 \\ 0 & 0 & 0 & \eta & \sigma\eta & \sigma & 0 & 0 & 0 & 0 & 0 & 0 & 0 & 0 & 0 & 0 & 0 & 0 & 0 & 0 & 0 & 0 & 0 & 0 & 0 & 0 & 0 \\ 0 & 0 & 0 & 0 & 0 & 0 & \nu & \sigma & \sigma\nu & 0 & 0 & 0 & 0 & 0 & 0 & 0 & 0 & 0 & 0 & 0 & 0 & 0 & 0 & 0 & 0 & 0 & 0 \\ 0 & 0 & 0 & 0 & 0 & 0 & 0 & 0 & 0 & 1 & \sigma & \sigma & 0 & 0 & 0 & 0 & 0 & 0 & 0 & 0 & 0 & 0 & 0 & 0 & 0 & 0 & 0 \\ 0 & 0 & 0 & 0 & 0 & 0 & 0 & 0 & 0 & 0 & 0 & 0 & 0 & \nu & \sigma\nu & \sigma & 0 & 0 & 0 & 0 & 0 & 0 & 0 & 0 & 0 & 0 & 0 \\ 0 & 0 & 0 & 0 & 0 & 0 & 0 & 0 & 0 & 0 & 0 & 0 & 0 & 0 & 0 & 0 & \omega & 0 & \sigma\omega & 0 & 0 & 0 & 0 & 0 & 0 & 0 & 0 \\ 0 & 0 & 0 & 0 & 0 & 0 & 0 & 0 & 0 & 0 & 0 & 0 & 0 & 0 & 0 & 0 & 0 & 0 & 0 & 1 & \sigma & \sigma & 0 & 0 & 0 & 0 & 0 \\ 0 & 0 & 0 & 0 & 0 & 0 & 0 & 0 & 0 & 0 & 0 & 0 & 0 & 0 & 0 & 0 & 0 & 0 & 0 & 0 & 0 & 0 & \omega & \sigma\omega & 0 & 0 & 0 \\ 0 & 0 & 0 & 0 & 0 & 0 & 0 & 0 & 0 & 0 & 0 & 0 & 0 & 0 & 0 & 0 & 0 & 0 & 0 & 0 & 0 & 0 & 0 & 0 & \eta & \sigma & \sigma\eta \end{pmatrix} \end{array}$$

(e)

$$U_4^{dd} = U_4^{dl} = \begin{array}{c} \\ t\ t \\ t\ g^+ \\ t\ g^- \\ g^+t \\ g^+g^+ \\ g^+g^- \\ g^-t \\ g^-g^+ \\ g^-g^- \end{array} \begin{array}{c} \begin{array}{ccccccccccccccccccccccccccc} t & g^+ & g^- & t & g^+ & g^- & t & g^+ & g^- & t & g^+ & g^- & t & g^+ & g^- & t & g^+ & g^- & t & g^+ & g^- & t & g^+ & g^- & t & g^+ & g^- \end{array} \\ \begin{pmatrix} 1 & \sigma & \sigma & 0 & 0 & 0 & 0 & 0 & 0 & 0 & 0 & 0 & 0 & 0 & 0 & 0 & 0 & 0 & 0 & 0 & 0 & 0 & 0 & 0 & 0 & 0 & 0 \\ 0 & 0 & 0 & \nu & \sigma\nu & \sigma & 0 & 0 & 0 & 0 & 0 & 0 & 0 & 0 & 0 & 0 & 0 & 0 & 0 & 0 & 0 & 0 & 0 & 0 & 0 & 0 & 0 \\ 0 & 0 & 0 & 0 & 0 & 0 & \eta & \sigma & \sigma\eta & 0 & 0 & 0 & 0 & 0 & 0 & 0 & 0 & 0 & 0 & 0 & 0 & 0 & 0 & 0 & 0 & 0 & 0 \\ 0 & 0 & 0 & 0 & 0 & 0 & 0 & 0 & 0 & 1 & \sigma & \sigma & 0 & 0 & 0 & 0 & 0 & 0 & 0 & 0 & 0 & 0 & 0 & 0 & 0 & 0 & 0 \\ 0 & 0 & 0 & 0 & 0 & 0 & 0 & 0 & 0 & 0 & 0 & 0 & 0 & \eta & \sigma\eta & \sigma & 0 & 0 & 0 & 0 & 0 & 0 & 0 & 0 & 0 & 0 & 0 \\ 0 & 0 & 0 & 0 & 0 & 0 & 0 & 0 & 0 & 0 & 0 & 0 & 0 & 0 & 0 & 0 & \omega & 0 & \sigma\omega & 0 & 0 & 0 & 0 & 0 & 0 & 0 & 0 \\ 0 & 0 & 0 & 0 & 0 & 0 & 0 & 0 & 0 & 0 & 0 & 0 & 0 & 0 & 0 & 0 & 0 & 0 & 0 & 1 & \sigma & \sigma & 0 & 0 & 0 & 0 & 0 \\ 0 & 0 & 0 & 0 & 0 & 0 & 0 & 0 & 0 & 0 & 0 & 0 & 0 & 0 & 0 & 0 & 0 & 0 & 0 & 0 & 0 & 0 & \omega & \sigma\omega & 0 & 0 & 0 \\ 0 & 0 & 0 & 0 & 0 & 0 & 0 & 0 & 0 & 0 & 0 & 0 & 0 & 0 & 0 & 0 & 0 & 0 & 0 & 0 & 0 & 0 & 0 & 0 & \nu & \sigma & \sigma\nu \end{pmatrix} \end{array}$$

Figure 12. Statistical weight matrices, $U_2 - U_4$, of di-MPDA and PTMI. The rows and columns are assigned to rotational states of the previous and current bonds, respectively. For example, the label on the second row of U_4, tg^+, indicates that bonds 2 and 3 adopt the trans and gauche$^+$ conformations, respectively.

The molecular parameters of PMTMI at 25 °C were calculated similarly. The $\langle r^2\rangle_0/nl^2$ vs x^{-1} curve for $n_c = 512$ also shows a monotonic decrease (Figure 10). The following data were obtained: $\langle r^2\rangle_0/nl^2 = 4.2$ at $x^{-1} = 0$, $10^3\, d \ln \langle r^2\rangle_0/dT = 1.5\ \mathrm{K}^{-1}$, $P_m = 0.48$, $p_t^{CC} = 0.40$, and $p_t^{CN} = 0.65$. Both PTMI and PMTMI chains are slightly rich in *racemo* configuration, whereas the PEI chain exhibits a comparatively strong *meso* preference ($P_m = 0.63$).[1,31] As the number of methylene units between the nitrogen atoms increases, the configuration may approach randomness ($P_m = P_r = 1/2$).

Listed in Table 8 are first derivatives of the characteristic ratio, *meso*-diad probability, and bond conformations of PTMI and PMTMI with respect to the conformational energies. The magnitude represents the sensitivity of the molecular parameter to the energy. For example, sizable $\partial(\langle r^2\rangle_0/nl^2)/\partial E_\xi$ values are found for E_σ, E_ν, E_η, and $E_{\psi''}$ of PTMI and E_σ and E_η of PMTMI; therefore, each variation significantly affects the spatial configuration of the polymer. The trans fractions are greatly affected by the first-order interaction(s) around the bond and the hydrogen bonds. In Figure 11, the molecular parameters are expressed as a function of E_σ or $E_{\psi''}$ for PTMI and E_σ or E_η for PMTMI because these energy parameters were found to be especially influential.

For PTMI, the N−H ··N hydrogen bond (ψ'' interaction) renders the C−C bond rich in gauche conformation. The shaded belts represent the p_t^{CC} and p_t^{CN} ranges determined from the NMR experiments for di-MPDA. The p_t^{CN} curves are included in the shaded area, whereas the p_t^{CC} curves overlap with the belt only around the energies larger than the MO calculations. The σ and ψ'' interactions may be subject to a solvent effect. As found for E_ω of PEO[28,37] and E_η and E_ν of PEI,[1] the right shift of $E_{\psi''}$ probably corresponds to an intramolecular-to-intermolecular transfer of the attractive interaction, leading to an increase in chain dimension and more random configuration. For PMTMI, E_σ and E_η behave as essentially equivalent variables for all the parameters. The p_t^{CC} vs E_η curve cuts across the experimental p_t^{CC} zone; the right shift of E_η suggests the solvent effect similar to those found for PEO, PEI, and PTMI.

The N−C−C−C−N unit corresponds to one generation of PTMI dendrimers. For linear PTMI and PMTMI, the C−N bond prefers the trans conformation ($p_t^{CN} \sim 0.65$−0.77), thus being rather rigid. On the other hand, the C−C bond is flexible: PTMI, $p_t^{CC} \sim 0.3$ and $p_{g+}^{CC} = p_{g-}^{CC} \sim 0.35$; PMTMI, $p_t^{CC} \sim 0.4$ and $p_{g+}^{CC} = p_{g-}^{CC} \sim 0.3$. The three rotational states are occupied to an approximately equal degree. In the dendrimer, the hyperbranching restricts the inversional-rotational isomerizations; the results here may not be directly apply to the dendrimers. Nevertheless, this study provides answers to prob-

(a)

$$U_5^{ll} = \begin{array}{c} \\ tt t \\ tt g^+ \\ tt g^- \\ t g^+t \\ t g^+g^+ \\ t g^+g^- \\ t g^-t \\ t g^-g^+ \\ t g^-g^- \\ g^+t\ t \\ g^+t\ g^+ \\ g^+t\ g^- \\ g^+g^+t \\ g^+g^+g^+ \\ g^+g^+g^- \\ g^+g^-t \\ g^+g^-g^+ \\ g^+g^-g^- \\ g^-t\ t \\ g^-t\ g^+ \\ g^-t\ g^- \\ g^-g^+t \\ g^-g^+g^+ \\ g^-g^+g^- \\ g^-g^-t \\ g^-g^-g^+ \\ g^-g^-g^- \end{array} \begin{array}{c} \begin{array}{cccccccccccccccccccccccccc} t & g^+ & g^- & t & g^+ & g^- & t & g^+ & g^- & t & g^+ & g^- & t & g^+ & g^- & t & g^+ & g^- & t & g^+ & g^- & t & g^+ & g^- & t & g^+ & g^- \end{array} \\ \begin{pmatrix} 1 & \delta & \gamma & 0 & 0 & 0 & 0 & 0 & 0 & 0 & 0 & 0 & 0 & 0 & 0 & 0 & 0 & 0 & 0 & 0 & 0 & 0 & 0 & 0 & 0 & 0 & 0 \\ 0 & 0 & 0 & \nu & \delta\eta & \gamma\omega & 0 & 0 & 0 & 0 & 0 & 0 & 0 & 0 & 0 & 0 & 0 & 0 & 0 & 0 & 0 & 0 & 0 & 0 & 0 & 0 & 0 \\ 0 & 0 & 0 & 0 & 0 & 0 & \eta & \delta\omega & \gamma\nu & 0 & 0 & 0 & 0 & 0 & 0 & 0 & 0 & 0 & 0 & 0 & 0 & 0 & 0 & 0 & 0 & 0 & 0 \\ 0 & 0 & 0 & 0 & 0 & 0 & 0 & 0 & 0 & 1 & \delta & \gamma & 0 & 0 & 0 & 0 & 0 & 0 & 0 & 0 & 0 & 0 & 0 & 0 & 0 & 0 & 0 \\ 0 & 0 & 0 & 0 & 0 & 0 & 0 & 0 & 0 & 0 & 0 & 0 & \nu & \delta\eta & \gamma\omega & 0 & 0 & 0 & 0 & 0 & 0 & 0 & 0 & 0 & 0 & 0 & 0 \\ 0 & 0 & 0 & 0 & 0 & 0 & 0 & 0 & 0 & 0 & 0 & 0 & 0 & 0 & 0 & \psi & 0 & \gamma\psi'' & 0 & 0 & 0 & 0 & 0 & 0 & 0 & 0 & 0 \\ 0 & 0 & 0 & 0 & 0 & 0 & 0 & 0 & 0 & 0 & 0 & 0 & 0 & 0 & 0 & 0 & 0 & 0 & 1 & \delta & \gamma & 0 & 0 & 0 & 0 & 0 & 0 \\ 0 & 0 & 0 & 0 & 0 & 0 & 0 & 0 & 0 & 0 & 0 & 0 & 0 & 0 & 0 & 0 & 0 & 0 & 0 & 0 & 0 & \psi' & \delta\psi'' & 0 & 0 & 0 & 0 \\ 0 & 0 & 0 & 0 & 0 & 0 & 0 & 0 & 0 & 0 & 0 & 0 & 0 & 0 & 0 & 0 & 0 & 0 & 0 & 0 & 0 & 0 & 0 & \eta & \delta\omega & \gamma\nu \\ 1 & \delta & \gamma & 0 & 0 & 0 & 0 & 0 & 0 & 0 & 0 & 0 & 0 & 0 & 0 & 0 & 0 & 0 & 0 & 0 & 0 & 0 & 0 & 0 & 0 & 0 & 0 \\ 0 & 0 & 0 & \nu & \delta\eta & \gamma\omega & 0 & 0 & 0 & 0 & 0 & 0 & 0 & 0 & 0 & 0 & 0 & 0 & 0 & 0 & 0 & 0 & 0 & 0 & 0 & 0 & 0 \\ 0 & 0 & 0 & 0 & 0 & 0 & \eta & \delta\omega & \gamma\nu & 0 & 0 & 0 & 0 & 0 & 0 & 0 & 0 & 0 & 0 & 0 & 0 & 0 & 0 & 0 & 0 & 0 & 0 \\ 0 & 0 & 0 & 0 & 0 & 0 & 0 & 0 & 0 & 1 & \delta & \gamma & 0 & 0 & 0 & 0 & 0 & 0 & 0 & 0 & 0 & 0 & 0 & 0 & 0 & 0 & 0 \\ 0 & 0 & 0 & 0 & 0 & 0 & 0 & 0 & 0 & 0 & 0 & 0 & \nu & \delta\eta & \gamma\omega & 0 & 0 & 0 & 0 & 0 & 0 & 0 & 0 & 0 & 0 & 0 & 0 \\ 0 & 0 & 0 & 0 & 0 & 0 & 0 & 0 & 0 & 0 & 0 & 0 & 0 & 0 & 0 & \psi'' & 0 & \gamma\psi' & 0 & 0 & 0 & 0 & 0 & 0 & 0 & 0 & 0 \\ 0 & 0 & 0 & 0 & 0 & 0 & 0 & 0 & 0 & 0 & 0 & 0 & 0 & 0 & 0 & 0 & 0 & 0 & 1 & \delta & \gamma & 0 & 0 & 0 & 0 & 0 & 0 \\ 0 & 0 & 0 & 0 & 0 & 0 & 0 & 0 & 0 & 0 & 0 & 0 & 0 & 0 & 0 & 0 & 0 & 0 & 0 & 0 & 0 & 0 & 0 & 0 & 0 & 0 & 0 \\ 0 & 0 & 0 & 0 & 0 & 0 & 0 & 0 & 0 & 0 & 0 & 0 & 0 & 0 & 0 & 0 & 0 & 0 & 0 & 0 & 0 & 0 & 0 & 0 & \eta & \delta\omega & \gamma\nu \\ 1 & \delta & \gamma & 0 & 0 & 0 & 0 & 0 & 0 & 0 & 0 & 0 & 0 & 0 & 0 & 0 & 0 & 0 & 0 & 0 & 0 & 0 & 0 & 0 & 0 & 0 & 0 \\ 0 & 0 & 0 & \nu & \delta\eta & \gamma\omega & 0 & 0 & 0 & 0 & 0 & 0 & 0 & 0 & 0 & 0 & 0 & 0 & 0 & 0 & 0 & 0 & 0 & 0 & 0 & 0 & 0 \\ 0 & 0 & 0 & 0 & 0 & 0 & \eta & \delta\omega & \gamma\nu & 0 & 0 & 0 & 0 & 0 & 0 & 0 & 0 & 0 & 0 & 0 & 0 & 0 & 0 & 0 & 0 & 0 & 0 \\ 0 & 0 & 0 & 0 & 0 & 0 & 0 & 0 & 0 & 1 & \delta & \gamma & 0 & 0 & 0 & 0 & 0 & 0 & 0 & 0 & 0 & 0 & 0 & 0 & 0 & 0 & 0 \\ 0 & 0 & 0 & 0 & 0 & 0 & 0 & 0 & 0 & 0 & 0 & 0 & \nu & 0 & \gamma\omega & 0 & 0 & 0 & 0 & 0 & 0 & 0 & 0 & 0 & 0 & 0 & 0 \\ 0 & 0 & 0 & 0 & 0 & 0 & 0 & 0 & 0 & 0 & 0 & 0 & 0 & 0 & 0 & 0 & 0 & 0 & 0 & 0 & 0 & 0 & 0 & 0 & 0 & 0 & 0 \\ 0 & 0 & 0 & 0 & 0 & 0 & 0 & 0 & 0 & 0 & 0 & 0 & 0 & 0 & 0 & 0 & 0 & 0 & 1 & \delta & \gamma & 0 & 0 & 0 & 0 & 0 & 0 \\ 0 & 0 & 0 & 0 & 0 & 0 & 0 & 0 & 0 & 0 & 0 & 0 & 0 & 0 & 0 & 0 & 0 & 0 & 0 & 0 & 0 & \psi'' & \delta\psi & 0 & 0 & 0 & 0 \\ 0 & 0 & 0 & 0 & 0 & 0 & 0 & 0 & 0 & 0 & 0 & 0 & 0 & 0 & 0 & 0 & 0 & 0 & 0 & 0 & 0 & 0 & 0 & \eta & 0 & \gamma\nu \end{pmatrix} \end{array}$$

(b)

$$U_5^{ld} = \begin{array}{c} \\ tt t \\ tt g^+ \\ tt g^- \\ t g^+t \\ t g^+g^+ \\ t g^+g^- \\ t g^-t \\ t g^-g^+ \\ t g^-g^- \\ g^+t\ t \\ g^+t\ g^+ \\ g^+t\ g^- \\ g^+g^+t \\ g^+g^+g^+ \\ g^+g^+g^- \\ g^+g^-t \\ g^+g^-g^+ \\ g^+g^-g^- \\ g^-t\ t \\ g^-t\ g^+ \\ g^-t\ g^- \\ g^-g^+t \\ g^-g^+g^+ \\ g^-g^+g^- \\ g^-g^-t \\ g^-g^-g^+ \\ g^-g^-g^- \end{array} \begin{array}{c} \begin{array}{cccccccccccccccccccccccccc} t & g^+ & g^- & t & g^+ & g^- & t & g^+ & g^- & t & g^+ & g^- & t & g^+ & g^- & t & g^+ & g^- & t & g^+ & g^- & t & g^+ & g^- & t & g^+ & g^- \end{array} \\ \begin{pmatrix} 1 & \gamma & \delta & 0 & 0 & 0 & 0 & 0 & 0 & 0 & 0 & 0 & 0 & 0 & 0 & 0 & 0 & 0 & 0 & 0 & 0 & 0 & 0 & 0 & 0 & 0 & 0 \\ 0 & 0 & 0 & \eta & \gamma\nu & \delta\omega & 0 & 0 & 0 & 0 & 0 & 0 & 0 & 0 & 0 & 0 & 0 & 0 & 0 & 0 & 0 & 0 & 0 & 0 & 0 & 0 & 0 \\ 0 & 0 & 0 & 0 & 0 & 0 & \nu & \gamma\omega & \delta\eta & 0 & 0 & 0 & 0 & 0 & 0 & 0 & 0 & 0 & 0 & 0 & 0 & 0 & 0 & 0 & 0 & 0 & 0 \\ 0 & 0 & 0 & 0 & 0 & 0 & 0 & 0 & 0 & 1 & \gamma & \delta & 0 & 0 & 0 & 0 & 0 & 0 & 0 & 0 & 0 & 0 & 0 & 0 & 0 & 0 & 0 \\ 0 & 0 & 0 & 0 & 0 & 0 & 0 & 0 & 0 & 0 & 0 & 0 & \eta & \gamma\nu & 0 & 0 & 0 & 0 & 0 & 0 & 0 & 0 & 0 & 0 & 0 & 0 & 0 \\ 0 & 0 & 0 & 0 & 0 & 0 & 0 & 0 & 0 & 0 & 0 & 0 & 0 & 0 & 0 & \psi'' & 0 & 0 & 0 & 0 & 0 & 0 & 0 & 0 & 0 & 0 & 0 \\ 0 & 0 & 0 & 0 & 0 & 0 & 0 & 0 & 0 & 0 & 0 & 0 & 0 & 0 & 0 & 0 & 0 & 0 & 1 & \gamma & \delta & 0 & 0 & 0 & 0 & 0 & 0 \\ 0 & 0 & 0 & 0 & 0 & 0 & 0 & 0 & 0 & 0 & 0 & 0 & 0 & 0 & 0 & 0 & 0 & 0 & 0 & 0 & 0 & \psi'' & \gamma\psi' & 0 & 0 & 0 & 0 \\ 0 & 0 & 0 & 0 & 0 & 0 & 0 & 0 & 0 & 0 & 0 & 0 & 0 & 0 & 0 & 0 & 0 & 0 & 0 & 0 & 0 & 0 & 0 & 0 & \nu & \gamma\omega & \delta\eta \\ 1 & \gamma & \delta & 0 & 0 & 0 & 0 & 0 & 0 & 0 & 0 & 0 & 0 & 0 & 0 & 0 & 0 & 0 & 0 & 0 & 0 & 0 & 0 & 0 & 0 & 0 & 0 \\ 0 & 0 & 0 & \eta & \gamma\nu & \delta\omega & 0 & 0 & 0 & 0 & 0 & 0 & 0 & 0 & 0 & 0 & 0 & 0 & 0 & 0 & 0 & 0 & 0 & 0 & 0 & 0 & 0 \\ 0 & 0 & 0 & 0 & 0 & 0 & \nu & \gamma\omega & \delta\eta & 0 & 0 & 0 & 0 & 0 & 0 & 0 & 0 & 0 & 0 & 0 & 0 & 0 & 0 & 0 & 0 & 0 & 0 \\ 0 & 0 & 0 & 0 & 0 & 0 & 0 & 0 & 0 & 1 & \gamma & \delta & 0 & 0 & 0 & 0 & 0 & 0 & 0 & 0 & 0 & 0 & 0 & 0 & 0 & 0 & 0 \\ 0 & 0 & 0 & 0 & 0 & 0 & 0 & 0 & 0 & 0 & 0 & 0 & \eta & \gamma\nu & 0 & 0 & 0 & 0 & 0 & 0 & 0 & 0 & 0 & 0 & 0 & 0 & 0 \\ 0 & 0 & 0 & 0 & 0 & 0 & 0 & 0 & 0 & 0 & 0 & 0 & 0 & 0 & 0 & \psi' & 0 & \delta\psi'' & 0 & 0 & 0 & 0 & 0 & 0 & 0 & 0 & 0 \\ 0 & 0 & 0 & 0 & 0 & 0 & 0 & 0 & 0 & 0 & 0 & 0 & 0 & 0 & 0 & 0 & 0 & 0 & 1 & \gamma & \delta & 0 & 0 & 0 & 0 & 0 & 0 \\ 0 & 0 & 0 & 0 & 0 & 0 & 0 & 0 & 0 & 0 & 0 & 0 & 0 & 0 & 0 & 0 & 0 & 0 & 0 & 0 & 0 & 0 & 0 & 0 & \nu & \gamma\omega & \delta\eta \\ 1 & \gamma & \delta & 0 & 0 & 0 & 0 & 0 & 0 & 0 & 0 & 0 & 0 & 0 & 0 & 0 & 0 & 0 & 0 & 0 & 0 & 0 & 0 & 0 & 0 & 0 & 0 \\ 0 & 0 & 0 & \eta & \gamma\nu & \delta\omega & 0 & 0 & 0 & 0 & 0 & 0 & 0 & 0 & 0 & 0 & 0 & 0 & 0 & 0 & 0 & 0 & 0 & 0 & 0 & 0 & 0 \\ 0 & 0 & 0 & 0 & 0 & 0 & \nu & \gamma\omega & \delta\eta & 0 & 0 & 0 & 0 & 0 & 0 & 0 & 0 & 0 & 0 & 0 & 0 & 0 & 0 & 0 & 0 & 0 & 0 \\ 0 & 0 & 0 & 0 & 0 & 0 & 0 & 0 & 0 & 1 & \gamma & \delta & 0 & 0 & 0 & 0 & 0 & 0 & 0 & 0 & 0 & 0 & 0 & 0 & 0 & 0 & 0 \\ 0 & 0 & 0 & 0 & 0 & 0 & 0 & 0 & 0 & 0 & 0 & 0 & 0 & 0 & \delta\omega & 0 & 0 & 0 & 0 & 0 & 0 & 0 & 0 & 0 & 0 & 0 & 0 \\ 0 & 0 & 0 & 0 & 0 & 0 & 0 & 0 & 0 & 0 & 0 & 0 & 0 & 0 & 0 & 0 & 0 & 0 & 0 & 0 & 0 & 0 & 0 & 0 & 0 & 0 & 0 \\ 0 & 0 & 0 & 0 & 0 & 0 & 0 & 0 & 0 & 0 & 0 & 0 & 0 & 0 & 0 & 0 & 0 & 0 & 1 & \gamma & \delta & 0 & 0 & 0 & 0 & 0 & 0 \\ 0 & 0 & 0 & 0 & 0 & 0 & 0 & 0 & 0 & 0 & 0 & 0 & 0 & 0 & 0 & 0 & 0 & 0 & 0 & 0 & 0 & \gamma\psi'' & 0 & 0 & 0 & 0 & 0 \\ 0 & 0 & 0 & 0 & 0 & 0 & 0 & 0 & 0 & 0 & 0 & 0 & 0 & 0 & 0 & 0 & 0 & 0 & 0 & 0 & 0 & 0 & 0 & \nu & \gamma\omega & \delta\eta \end{pmatrix} \end{array}$$

Figure 13. Statistical weight matrices, U_5^{ll} and U_5^{ld}, of di-MPDA and PTMI. The rows and columns are assigned to rotational states of the previous and current bonds, respectively. For example, the label on the sixth row, tg^+g^-, indicates that bonds 2, 3, and 4 adopt the trans, gauche$^+$, and gauche$^-$ conformations, respectively.

lems disputed so far about PTMI dendrimers: [38−41] The backfolding due to the flexible C−C bond frequently occurs, the terminal NH_2 groups can be anchored to the inner sites by the N−H···N and C−H···N hydrogen bonds, and the spatial configuration depends on solvent owing to the transfer of the attractive interactions.

4. Concluding Remarks

Conformations, configurations, and solution properties of PTMI and PMTMI have been well characterized by the IRIS analysis of ab initio MO calculations and NMR experiments for the model compounds. We have thus far found two types of weak hydrogen bonds in

(a)

$$U_{\mathrm{a}}^{ll} = U_{\mathrm{a}}^{ld} =$$

	t	g^+	g^-	t	g^+	g^-	t	g^+	g^-	t	g^+	g^-	t	g^+	g^-	t	g^+	g^-	t	g^+	g^-	t	g^+	g^-	t	g^+	g^-
$t\ t\ t$	1	γ	δ	0	0	0	0	0	0	0	0	0	0	0	0	0	0	0	0	0	0	0	0	0	0	0	0	0
$t\ t\ g^+$	0	0	0	1	γ	$\delta\omega'$	0	0	0	0	0	0	0	0	0	0	0	0	0	0	0	0	0	0	0	0	0	0
$t\ t\ g^-$	0	0	0	0	0	0	1	$\gamma\omega'$	δ	0	0	0	0	0	0	0	0	0	0	0	0	0	0	0	0	0	0	0
$t\ g^+t$	0	0	0	0	0	0	0	0	0	1	γ	δ	0	0	0	0	0	0	0	0	0	0	0	0	0	0	0	0
$t\ g^+g^+$	0	0	0	0	0	0	0	0	0	0	0	0	1	γ	$\delta\omega'$	0	0	0	0	0	0	0	0	0	0	0	0	0
$t\ g^+g^-$	0	0	0	0	0	0	0	0	0	0	0	0	0	0	0	1	0	δ	0	0	0	0	0	0	0	0	0	0
$t\ g^-t$	0	0	0	0	0	0	0	0	0	0	0	0	0	0	0	0	0	0	1	γ	δ	0	0	0	0	0	0	0
$t\ g^-g^+$	0	0	0	0	0	0	0	0	0	0	0	0	0	0	0	0	0	0	0	0	0	1	γ	0	0	0	0	0
$t\ g^-g^-$	0	0	0	0	0	0	0	0	0	0	0	0	0	0	0	0	0	0	0	0	0	0	0	0	1	$\gamma\omega'$	δ	0
$g^+t\ t$	1	γ	δ	0	0	0	0	0	0	0	0	0	0	0	0	0	0	0	0	0	0	0	0	0	0	0	0	0
$g^+t\ g^+$	0	0	0	1	γ	$\delta\omega'$	0	0	0	0	0	0	0	0	0	0	0	0	0	0	0	0	0	0	0	0	0	0
$g^+t\ g^-$	0	0	0	0	0	0	1	$\gamma\omega'$	δ	0	0	0	0	0	0	0	0	0	0	0	0	0	0	0	0	0	0	0
g^+g^+t	0	0	0	0	0	0	0	0	0	0	1	γ	δ	0	0	0	0	0	0	0	0	0	0	0	0	0	0	0
$g^+g^+g^+$	0	0	0	0	0	0	0	0	0	0	0	0	0	1	γ	$\delta\omega'$	0	0	0	0	0	0	0	0	0	0	0	0
$g^+g^+g^-$	0	0	0	0	0	0	0	0	0	0	0	0	0	0	0	0	1	0	δ	0	0	0	0	0	0	0	0	0
g^+g^-t	0	0	0	0	0	0	0	0	0	0	0	0	0	0	0	0	0	0	0	1	γ	δ	0	0	0	0	0	0
$g^+g^-g^+$	0	0	0	0	0	0	0	0	0	0	0	0	0	0	0	0	0	0	0	0	1	γ	0	0	0	0	0	0
$g^+g^-g^-$	0	0	0	0	0	0	0	0	0	0	0	0	0	0	0	0	0	0	0	0	0	0	1	$\gamma\omega'$	δ	0	0	0
$g^-t\ t$	1	γ	δ	0	0	0	0	0	0	0	0	0	0	0	0	0	0	0	0	0	0	0	0	0	0	0	0	0
$g^-t\ g^+$	0	0	0	1	γ	$\delta\omega'$	0	0	0	0	0	0	0	0	0	0	0	0	0	0	0	0	0	0	0	0	0	0
$g^-t\ g^-$	0	0	0	0	0	0	1	$\gamma\omega'$	δ	0	0	0	0	0	0	0	0	0	0	0	0	0	0	0	0	0	0	0
g^-g^+t	0	0	0	0	0	0	0	0	0	0	1	γ	δ	0	0	0	0	0	0	0	0	0	0	0	0	0	0	0
$g^-g^+g^+$	0	0	0	0	0	0	0	0	0	0	0	0	0	1	γ	$\delta\omega'$	0	0	0	0	0	0	0	0	0	0	0	0
$g^-g^+g^-$	0	0	0	0	0	0	0	0	0	0	0	0	0	0	0	0	1	0	δ	0	0	0	0	0	0	0	0	0
g^-g^-t	0	0	0	0	0	0	0	0	0	0	0	0	0	0	0	0	0	0	0	1	γ	δ	0	0	0	0	0	0
$g^-g^-g^+$	0	0	0	0	0	0	0	0	0	0	0	0	0	0	0	0	0	0	0	0	1	γ	0	0	0	0	0	0
$g^-g^-g^-$	0	0	0	0	0	0	0	0	0	0	0	0	0	0	0	0	0	0	0	0	0	0	1	$\gamma\omega'$	δ	0	0	0

(b)

$$U_{\mathrm{b}}^{ll} = U_{\mathrm{b}}^{ld} =$$

	t	g^+	g^-	t	g^+	g^-	t	g^+	g^-	t	g^+	g^-	t	g^+	g^-	t	g^+	g^-	t	g^+	g^-	t	g^+	g^-	t	g^+	g^-
$t\ t\ t$	1	σ	σ	0	0	0	0	0	0	0	0	0	0	0	0	0	0	0	0	0	0	0	0	0	0	0	0	0
$t\ t\ g^+$	0	0	0	1	σ	σ	0	0	0	0	0	0	0	0	0	0	0	0	0	0	0	0	0	0	0	0	0	0
$t\ t\ g^-$	0	0	0	0	0	0	1	σ	σ	0	0	0	0	0	0	0	0	0	0	0	0	0	0	0	0	0	0	0
$t\ g^+t$	0	0	0	0	0	0	0	0	0	1	σ	σ	0	0	0	0	0	0	0	0	0	0	0	0	0	0	0	0
$t\ g^+g^+$	0	0	0	0	0	0	0	0	0	0	0	0	1	σ	σ	0	0	0	0	0	0	0	0	0	0	0	0	0
$t\ g^+g^-$	0	0	0	0	0	0	0	0	0	0	0	0	0	0	0	1	0	σ	0	0	0	0	0	0	0	0	0	0
$t\ g^-t$	0	0	0	0	0	0	0	0	0	0	0	0	0	0	0	0	0	0	1	σ	σ	0	0	0	0	0	0	0
$t\ g^-g^+$	0	0	0	0	0	0	0	0	0	0	0	0	0	0	0	0	0	0	0	0	0	1	σ	0	0	0	0	0
$t\ g^-g^-$	0	0	0	0	0	0	0	0	0	0	0	0	0	0	0	0	0	0	0	0	0	0	0	0	1	σ	σ	0
$g^+t\ t$	1	σ	σ	0	0	0	0	0	0	0	0	0	0	0	0	0	0	0	0	0	0	0	0	0	0	0	0	0
$g^+t\ g^+$	0	0	0	1	σ	σ	0	0	0	0	0	0	0	0	0	0	0	0	0	0	0	0	0	0	0	0	0	0
$g^+t\ g^-$	0	0	0	0	0	0	1	σ	σ	0	0	0	0	0	0	0	0	0	0	0	0	0	0	0	0	0	0	0
g^+g^+t	0	0	0	0	0	0	0	0	0	0	1	σ	σ	0	0	0	0	0	0	0	0	0	0	0	0	0	0	0
$g^+g^+g^+$	0	0	0	0	0	0	0	0	0	0	0	0	1	σ	σ	0	0	0	0	0	0	0	0	0	0	0	0	0
$g^+g^+g^-$	0	0	0	0	0	0	0	0	0	0	0	0	0	1	σ	0	0	0	0	0	0	0	0	0	0	0	0	0
g^+g^-t	0	0	0	0	0	0	0	0	0	0	0	0	0	0	0	0	1	σ	σ	0	0	0	0	0	0	0	0	0
$g^+g^-g^+$	0	0	0	0	0	0	0	0	0	0	0	0	0	0	0	0	0	0	0	0	1	σ	0	0	0	0	0	0
$g^+g^-g^-$	0	0	0	0	0	0	0	0	0	0	0	0	0	0	0	0	0	0	0	0	0	1	σ	σ	0	0	0	0
$g^-t\ t$	1	σ	σ	0	0	0	0	0	0	0	0	0	0	0	0	0	0	0	0	0	0	0	0	0	0	0	0	0
$g^-t\ g^+$	0	0	0	1	σ	σ	0	0	0	0	0	0	0	0	0	0	0	0	0	0	0	0	0	0	0	0	0	0
$g^-t\ g^-$	0	0	0	0	0	0	1	σ	σ	0	0	0	0	0	0	0	0	0	0	0	0	0	0	0	0	0	0	0
g^-g^+t	0	0	0	0	0	0	0	0	0	0	1	σ	σ	0	0	0	0	0	0	0	0	0	0	0	0	0	0	0
$g^-g^+g^+$	0	0	0	0	0	0	0	0	0	0	0	0	0	1	σ	σ	0	0	0	0	0	0	0	0	0	0	0	0
$g^-g^+g^-$	0	0	0	0	0	0	0	0	0	0	0	0	0	0	0	0	1	0	σ	0	0	0	0	0	0	0	0	0
g^-g^-t	0	0	0	0	0	0	0	0	0	0	0	0	0	0	0	0	0	0	0	1	σ	σ	0	0	0	0	0	0
$g^-g^-g^+$	0	0	0	0	0	0	0	0	0	0	0	0	0	0	0	0	0	0	0	0	1	σ	0	0	0	0	0	0
$g^-g^-g^-$	0	0	0	0	0	0	0	0	0	0	0	0	0	0	0	0	0	0	0	0	0	1	σ	σ	0	0	0	0

(c)

$$U_{\mathrm{c}}^{ll} = U_{\mathrm{c}}^{ld} =$$

	t	g^+	g^-	t	g^+	g^-	t	g^+	g^-	t	g^+	g^-	t	g^+	g^-	t	g^+	g^-	t	g^+	g^-	t	g^+	g^-	t	g^+	g^-
$t\ t\ t$	1	σ	σ	0	0	0	0	0	0	0	0	0	0	0	0	0	0	0	0	0	0	0	0	0	0	0	0	0
$t\ t\ g^+$	0	0	0	η	$\sigma\eta$	σ	0	0	0	0	0	0	0	0	0	0	0	0	0	0	0	0	0	0	0	0	0	0
$t\ t\ g^-$	0	0	0	0	0	0	ν	σ	$\sigma\nu$	0	0	0	0	0	0	0	0	0	0	0	0	0	0	0	0	0	0	0
$t\ g^+t$	0	0	0	0	0	0	0	0	0	1	σ	σ	0	0	0	0	0	0	0	0	0	0	0	0	0	0	0	0
$t\ g^+g^+$	0	0	0	0	0	0	0	0	0	0	0	0	ν	$\sigma\nu$	σ	0	0	0	0	0	0	0	0	0	0	0	0	0
$t\ g^+g^-$	0	0	0	0	0	0	0	0	0	0	0	0	0	0	0	ω	0	$\sigma\omega$	0	0	0	0	0	0	0	0	0	0
$t\ g^-t$	0	0	0	0	0	0	0	0	0	0	0	0	0	0	0	0	0	0	1	σ	σ	0	0	0	0	0	0	0
$t\ g^-g^+$	0	0	0	0	0	0	0	0	0	0	0	0	0	0	0	0	0	0	0	0	0	ω	$\sigma\omega$	0	0	0	0	0
$t\ g^-g^-$	0	0	0	0	0	0	0	0	0	0	0	0	0	0	0	0	0	0	0	0	0	0	0	0	η	σ	$\sigma\eta$	0
$g^+t\ t$	1	σ	σ	0	0	0	0	0	0	0	0	0	0	0	0	0	0	0	0	0	0	0	0	0	0	0	0	0
$g^+t\ g^+$	0	0	0	η	$\sigma\eta$	σ	0	0	0	0	0	0	0	0	0	0	0	0	0	0	0	0	0	0	0	0	0	0
$g^+t\ g^-$	0	0	0	0	0	0	ν	σ	$\sigma\nu$	0	0	0	0	0	0	0	0	0	0	0	0	0	0	0	0	0	0	0
g^+g^+t	0	0	0	0	0	0	0	0	0	1	σ	σ	0	0	0	0	0	0	0	0	0	0	0	0	0	0	0	0
$g^+g^+g^+$	0	0	0	0	0	0	0	0	0	0	0	0	ν	$\sigma\nu$	σ	0	0	0	0	0	0	0	0	0	0	0	0	0
$g^+g^+g^-$	0	0	0	0	0	0	0	0	0	0	0	0	0	0	0	ω	0	$\sigma\omega$	0	0	0	0	0	0	0	0	0	0
g^+g^-t	0	0	0	0	0	0	0	0	0	0	0	0	0	0	0	0	0	0	0	1	σ	σ	0	0	0	0	0	0
$g^+g^-g^+$	0	0	0	0	0	0	0	0	0	0	0	0	0	0	0	0	0	0	0	0	0	ω	$\sigma\omega$	0	0	0	0	0
$g^+g^-g^-$	0	0	0	0	0	0	0	0	0	0	0	0	0	0	0	0	0	0	0	0	0	0	0	0	η	σ	$\sigma\eta$	0
$g^-t\ t$	1	σ	σ	0	0	0	0	0	0	0	0	0	0	0	0	0	0	0	0	0	0	0	0	0	0	0	0	0
$g^-t\ g^+$	0	0	0	η	$\sigma\eta$	σ	0	0	0	0	0	0	0	0	0	0	0	0	0	0	0	0	0	0	0	0	0	0
$g^-t\ g^-$	0	0	0	0	0	0	ν	σ	$\sigma\nu$	0	0	0	0	0	0	0	0	0	0	0	0	0	0	0	0	0	0	0
g^-g^+t	0	0	0	0	0	0	0	0	0	1	σ	σ	0	0	0	0	0	0	0	0	0	0	0	0	0	0	0	0
$g^-g^+g^+$	0	0	0	0	0	0	0	0	0	0	0	0	ν	$\sigma\nu$	σ	0	0	0	0	0	0	0	0	0	0	0	0	0
$g^-g^+g^-$	0	0	0	0	0	0	0	0	0	0	0	0	0	0	0	ω	0	$\sigma\omega$	0	0	0	0	0	0	0	0	0	0
g^-g^-t	0	0	0	0	0	0	0	0	0	0	0	0	0	0	0	0	0	0	0	1	σ	σ	0	0	0	0	0	0
$g^-g^-g^+$	0	0	0	0	0	0	0	0	0	0	0	0	0	0	0	0	0	0	0	0	0	ω	$\sigma\omega$	0	0	0	0	0
$g^-g^-g^-$	0	0	0	0	0	0	0	0	0	0	0	0	0	0	0	0	0	0	0	0	0	0	0	0	η	σ	$\sigma\eta$	0

Figure 14. Statistical weight matrices, U_{a}–U_{c}, of *ll* and *ld* repeating units of PTMI. The rows and columns are assigned to rotational states of the previous and current (jth) bonds, respectively. For example, the label on the sixth row, tg^+g^-, indicates that the $(j-3)$th, $(j-2)$th, and $(j-1)$th bonds adopt the trans, gauche$^+$, and gauche$^-$ conformations, respectively.

(a)

$$U_2^{ll} = U_2^{ld} = \begin{array}{c} \\ t \\ g^+ \\ g^- \end{array} \begin{array}{c} \begin{array}{ccc} t & g^+ & g^- \end{array} \\ \begin{pmatrix} 1 & \gamma & 1 \\ 0 & 0 & 0 \\ 0 & 0 & 0 \end{pmatrix} \end{array}$$

(b)

$$U_2^{dd} = U_2^{dl} = \begin{array}{c} \\ t \\ g^+ \\ g^- \end{array} \begin{array}{c} \begin{array}{ccc} t & g^+ & g^- \end{array} \\ \begin{pmatrix} 1 & 1 & \gamma \\ 0 & 0 & 0 \\ 0 & 0 & 0 \end{pmatrix} \end{array}$$

(c)

$$U_3^{ll} = U_3^{dd} = U_3^{ld} = U_3^{dl} = \begin{array}{c} \\ t \\ g^+ \\ g^- \end{array} \begin{array}{c} \begin{array}{ccccccccc} t & g^+ & g^- & t & g^+ & g^- & t & g^+ & g^- \end{array} \\ \begin{pmatrix} 1 & \sigma & \sigma & 0 & 0 & 0 & 0 & 0 & 0 \\ 0 & 0 & 0 & 1 & \sigma & \sigma & 0 & 0 & 0 \\ 0 & 0 & 0 & 0 & 0 & 0 & 1 & \sigma & \sigma \end{pmatrix} \end{array}$$

(d)

$$U_4^{ll} = U_4^{ld} = \begin{array}{c} \\ t\ t \\ t\ g^+ \\ t\ g^- \\ g^+t \\ g^+g^+ \\ g^+g^- \\ g^-t \\ g^-g^+ \\ g^-g^- \end{array} \begin{array}{c} \begin{array}{ccccccccc} t & g^+ & g^- & t & g^+ & g^- & t & g^+ & g^- \end{array} \\ \begin{pmatrix} 1 & \sigma & \sigma & 0 & 0 & 0 & 0 & 0 & 0 \\ 0 & 0 & 0 & \eta & \sigma\eta & \sigma & 0 & 0 & 0 \\ 0 & 0 & 0 & 0 & 0 & 0 & \omega & 0 & \sigma\omega \\ 1 & \sigma & \sigma & 0 & 0 & 0 & 0 & 0 & 0 \\ 0 & 0 & 0 & \omega & \sigma\omega & \sigma & 0 & 0 & 0 \\ 0 & 0 & 0 & 0 & 0 & 0 & \omega & 0 & \sigma\omega \\ 1 & \sigma & \sigma & 0 & 0 & 0 & 0 & 0 & 0 \\ 0 & 0 & 0 & \omega & \sigma\omega & 0 & 0 & 0 & 0 \\ 0 & 0 & 0 & 0 & 0 & 0 & \eta & \sigma & \sigma\eta \end{pmatrix} \end{array}$$

(e)

$$U_5^{ll} = \begin{array}{c} \\ t\ t \\ t\ g^+ \\ t\ g^- \\ g^+t \\ g^+g^+ \\ g^+g^- \\ g^-t \\ g^-g^+ \\ g^-g^- \end{array} \begin{array}{c} \begin{array}{ccccccccc} t & g^+ & g^- & t & g^+ & g^- & t & g^+ & g^- \end{array} \\ \begin{pmatrix} 1 & 1 & \gamma & 0 & 0 & 0 & 0 & 0 & 0 \\ 0 & 0 & 0 & \omega & \eta & \gamma\omega & 0 & 0 & 0 \\ 0 & 0 & 0 & 0 & 0 & 0 & \eta & \omega & \gamma\omega \\ 1 & 1 & \gamma & 0 & 0 & 0 & 0 & 0 & 0 \\ 0 & 0 & 0 & \omega & \eta & \gamma\omega & 0 & 0 & 0 \\ 0 & 0 & 0 & 0 & 0 & 0 & 0 & 0 & 0 \\ 1 & 1 & \gamma & 0 & 0 & 0 & 0 & 0 & 0 \\ 0 & 0 & 0 & 0 & 0 & 0 & 0 & 0 & 0 \\ 0 & 0 & 0 & 0 & 0 & 0 & \eta & \omega & \gamma\omega \end{pmatrix} \end{array}$$

(f)

$$U_5^{ld} = \begin{array}{c} \\ t\ t \\ t\ g^+ \\ t\ g^- \\ g^+t \\ g^+g^+ \\ g^+g^- \\ g^-t \\ g^-g^+ \\ g^-g^- \end{array} \begin{array}{c} \begin{array}{ccccccccc} t & g^+ & g^- & t & g^+ & g^- & t & g^+ & g^- \end{array} \\ \begin{pmatrix} 1 & \gamma & 1 & 0 & 0 & 0 & 0 & 0 & 0 \\ 0 & 0 & 0 & \eta & \gamma\omega & \omega & 0 & 0 & 0 \\ 0 & 0 & 0 & 0 & 0 & 0 & \omega & \gamma\omega & \eta \\ 1 & \gamma & 1 & 0 & 0 & 0 & 0 & 0 & 0 \\ 0 & 0 & 0 & \eta & \gamma\omega & \omega & 0 & 0 & 0 \\ 0 & 0 & 0 & 0 & 0 & 0 & 0 & 0 & 0 \\ 1 & \gamma & 1 & 0 & 0 & 0 & 0 & 0 & 0 \\ 0 & 0 & 0 & 0 & 0 & 0 & 0 & 0 & 0 \\ 0 & 0 & 0 & 0 & 0 & 0 & \omega & \gamma\omega & \eta \end{pmatrix} \end{array}$$

Figure 15. Statistical weight matrices, U_2–U_5, of tetra-MPDA and PMTMI.

polyimines: N–H···N of PEI and PTMI; C–H···N of PTMI and PMTMI. The former energies are −1.54 kcal mol^{-1} (the η interaction of PEI), −0.83 kcal mol^{-1} (ψ'' of PTMI), and −0.58 kcal mol^{-1} (ν of PEI), and the latter energies are −0.40 kcal mol^{-1} (η of PMTMI) and −0.15 kcal mol^{-1} (η of PTMI). Although such weak hydrogen bonds have been found in molecular crystals and supermolecules,[42,43] this study has shown that the attractive interactions significantly affect structures and properties of the polyimines undergoing rapid molecular motions.

In previous studies, we found weak (C–H)···O hydrogen bonds and evaluated the interaction energies as −1.3 to −1.1 kcal mol^{-1} (ω of PEO),[28,37,44,45] −1.24 kcal mol^{-1} (ω_1 of PPO), and −1.88 kcal mol^{-1} (ω_2 of PPO).[37,46] On the basis of theoretical and experimental results accumulated, we can conclude that the weak intramolecular and intermolecular attractions due to the heteroatoms are principal factors in the conformation, (configuration for polyimines), crystal structure, and solution properties of the polymers.

(a)

$$U_{\mathrm{a}}^{ll} = U_{\mathrm{a}}^{ld} = \begin{array}{c} \\ t\ t \\ t\ g^+ \\ t\ g^- \\ g^+t \\ g^+g^+ \\ g^+g^- \\ g^-t \\ g^-g^+ \\ g^-g^- \end{array} \begin{array}{c} \begin{array}{ccccccccc} t & g^+ & g^- & t & g^+ & g^- & t & g^+ & g^- \end{array} \\ \begin{pmatrix} 1 & \gamma & 1 & 0 & 0 & 0 & 0 & 0 & 0 \\ 0 & 0 & 0 & 1 & \gamma & 0 & 0 & 0 & 0 \\ 0 & 0 & 0 & 0 & 0 & 0 & 1 & \gamma\omega' & 1 \\ 1 & \gamma & 1 & 0 & 0 & 0 & 0 & 0 & 0 \\ 0 & 0 & 0 & 1 & \gamma & 0 & 0 & 0 & 0 \\ 0 & 0 & 0 & 0 & 0 & 0 & 1 & 0 & 1 \\ 1 & \gamma & 1 & 0 & 0 & 0 & 0 & 0 & 0 \\ 0 & 0 & 0 & 1 & \gamma & 0 & 0 & 0 & 0 \\ 0 & 0 & 0 & 0 & 0 & 0 & 1 & \gamma\omega' & 1 \end{pmatrix} \end{array}$$

(b)

$$U_{\mathrm{b}}^{ll} = U_b^{dd} = U_b^{ld} = U_b^{dl} = \begin{array}{c} \\ t\ t \\ t\ g^+ \\ t\ g^- \\ g^+t \\ g^+g^+ \\ g^+g^- \\ g^-t \\ g^-g^+ \\ g^-g^- \end{array} \begin{array}{c} \begin{array}{ccccccccc} t & g^+ & g^- & t & g^+ & g^- & t & g^+ & g^- \end{array} \\ \begin{pmatrix} 1 & \sigma & \sigma & 0 & 0 & 0 & 0 & 0 & 0 \\ 0 & 0 & 0 & 1 & \sigma & \sigma & 0 & 0 & 0 \\ 0 & 0 & 0 & 0 & 0 & 0 & 1 & \sigma & \sigma \\ 1 & \sigma & \sigma & 0 & 0 & 0 & 0 & 0 & 0 \\ 0 & 0 & 0 & 1 & \sigma & \sigma & 0 & 0 & 0 \\ 0 & 0 & 0 & 0 & 0 & 0 & 1 & 0 & \sigma \\ 1 & \sigma & \sigma & 0 & 0 & 0 & 0 & 0 & 0 \\ 0 & 0 & 0 & 1 & \sigma & 0 & 0 & 0 & 0 \\ 0 & 0 & 0 & 0 & 0 & 0 & 1 & \sigma & \sigma \end{pmatrix} \end{array}$$

Figure 16. Statistical weight matrices, U_{a} and U_{b}, of PMTMI.

Acknowledgment. On November 21, 2004, Professor Ichitaro Uematsu, a leading polymer scientist of Japan, passed away peacefully. He had led us to polymer science and continued to encourage us. This work was partly supported by the Asahi Glass Foundation.

Appendix. Statistical Weight Matrices of di-MPDA, PTMI, tetra-MPDA, and PMTMI

The U_2–U_5 matrices of di-MPDA and PTMI are shown in Figures 12 and 13. The U_{a}–U_{c} matrices of *ll* and *ld* repeating units of PTMI are given in Figure 14, and those of the *dd* and *dl* units can be derived from eqs 12 and 13, respectively. The U_2–U_5 matrices of tetra-MPDA and PMTMI and U_{a} and U_{b} of PMTMI are shown in Figures 15 and 16, respectively. The U_{c}^{α} and U_{d}^{α} matrices of PMTMI are equal to U_4^{α} and U_5^{α}, respectively ($\alpha = ll$, dd, ld, and dl). The U_4, U_5, and U_{a}–U_{d} matrices of *dd* and *dl* units of PMTMI (tetra-MPDA) are derived from

$$U_\beta^{dd} = Q_9 U_\beta^{ll} Q_9 \tag{A1}$$

and

$$U_\beta^{dl} = Q_9 U_\beta^{ld} Q_9 \tag{A2}$$

where β stands for the bond number, and Q_9 is given by

$$Q_9 = Q_3 \otimes Q_3 \tag{A3}$$

The Q_9 matrix is identical to Q of ref 1.

Supporting Information Available: Tables of ^{1}H and ^{13}C NMR vicinal coupling constants and conformer free energies of tri-MPDA and tetra-MPDA. This material is available free of charge via the Internet at http://pubs.acs.org.

References and Notes

(1) Sasanuma, Y.; Hattori, S.; Imazu, S.; Ikeda, S.; Kaizuka, T.; Iijima, T.; Sawanobori, M.; Azam, M. A.; Law, R. V.; Steinke, J. H. *Macromolecules* **2004**, *37*, 9169.
(2) Flory, P. J. *Statistical Mechanics of Chain Molecules;* Interscience: New York, 1969.
(3) Mattice, W. L.; Suter, U. W. *Conformational Theory of Large Molecules: The Rotational Isomeric State Model in Macromolecular Systems*; Wiley & Sons: New York, 1994.

(4) Levy, A.; Litt, M. *J. Polym. Sci., Polym. Lett. Ed.* **1967**, *5*, 881.

(5) Saegusa, T.; Nagura, Y.; Kobayashi, S. *Macromolecules* **1973**, *6*, 495.

(6) Saegusa, T.; Kobayashi, S.; Nagura, Y. *Macromolecules* **1974**, *7*, 265.

(7) Saegusa, T.; Kobayashi, S.; Nagura, Y. *Macromolecules* **1974**, *7*, 272.

(8) Saegusa, T.; Kobayashi, S.; Nagura, Y. *Macromolecules* **1974**, *7*, 713.

(9) Overberger, C. G.; Chang, J. Y.; Gunn, V. E. *J. Polym. Sci., Part A: Polym. Chem.* **1989**, *27*, 99.

(10) Linear PTMI is crystalline, very hygroscopic, soluble in chloroform, methanol, ethanol, and toluene, and insoluble in dimethylformamide, DMSO, and hot water. Its melting point, depending on the water content, varies from 74 to 84 °C.[5,9]

(11) The dendrimers have usually been referred to as poly(propylene imine) dendrimers. In this paper, however, the designation of poly(trimethylene imine) (PTMI) is used exclusively. In contrast to the linear polyimines, the dendrimers are soluble in a variety of solvents.

(12) Tomalia, D. A.; Baker, H.; Dewald, J.; Hall, M.; Kallos, G.; Martin, S.; Roeck, J.; Ryder, J.; Smith, P. *Polym. J.* **1985**, *17*, 117.

(13) Tomalia, D. A.; Naylor, A. M.; Goddard, W. A., III. *Angew. Chem., Int. Ed. Engl.* **1990**, *29*, 138.

(14) Bosman, A. W.; Janssen, H. M.; Meijer, E. W. *Chem. Rev.* **1999**, *99*, 1665.

(15) Frisch, M. J.; Trucks, G. W.; Schlegel, H. B.; Scuseria, G. E.; Robb, M. A.; Cheeseman, J. R.; Zakrzewski, V. G.; Montgomery, J. A., Jr.; Stratmann, R. E.; Burant, J. C.; Dapprich, S.; Millam, J. M.; Daniels, A. D.; Kudin, K. N.; Strain, M. C.; Farkas, O.; Tomasi, J.; Barone, V.; Cossi, M.; Cammi, R.; Mennucci, B.; Pomelli, C.; Adamo, C.; Clifford, S.; Ochterski, J.; Petersson, G. A.; Ayala, P. Y.; Cui, Q.; Morokuma, K.; Salvador, P.; Dannenberg, J. J.; Malick, D. K.; Rabuck, A. D.; Raghavachari, K.; Foresman, J. B.; Cioslowski, J.; Ortiz, J. V.; Baboul, A. G.; Stefanov, B. B.; Liu, G.; Liashenko, A.; Piskorz, P.; Komaromi, I.; Gomperts, R.; Martin, R. L.; Fox, D. J.; Keith, T.; Al-Laham, M. A.; Peng, C. Y.; Nanayakkara, A.; Challacombe, M.; Gill, P. M. W.; Johnson, B.; Chen, W.; Wong, M. W.; Andres, J. L.; Gonzalez, C.; Head-Gordon, M.; Replogle, E. S.; Pople, J. A. *Gaussian 98*, revision A.11. Gaussian, Inc.: Pittsburgh, PA, 2001.

(16) Foresman, J. B.; Frisch, A. E. *Exploring Chemistry with Electronic Structure Methods*, 2nd ed.; Gaussian, Inc.: Pittsburgh, PA, 1996.

(17) Frisch, M. J.; Trucks, G. W.; Schlegel, H. B.; Scuseria, G. E.; Robb, M. A.; Cheeseman, J. R.; Montgomery, J. A., Jr.; Vreven, T.; Kudin, K. N.; Burant, J. C.; Millam, J. M.; Iyengar, S. S.; Tomasi, J.; Barone, V.; Mennucci, B.; Cossi, M.; Scalmani, G.; Rega, N.; Petersson, G. A.; Nakatsuji, H.; Hada, M.; Ehara, M.; Toyota, K.; Fukuda, R.; Hasegawa, J.; Ishida, M.; Nakajima, T.; Honda, Y.; Kitao, O.; Nakai, H.; Klene, M.; Li, X.; Knox, J. E.; Hratchian, H. P.; Cross, J. B.; Bakken, V.; Adamo, C.; Jaramillo, J.; Gomperts, R.; Stratmann, R. E.; Yazyev, O.; Austin, A. J.; Cammi, R.; Pomelli, C.; Ochterski, J. W.; Ayala, P. Y.; Morokuma, K.; Voth, G. A.; Salvador, P.; Dannenberg, J. J.; Zakrzewski, V. G.; Dapprich, S.; Daniels, A. D.; Strain, M. C.; Farkas, O.; Malick, D. K.; Rabuck, A. D.; Raghavachari, K.; Foresman, J. B.; Ortiz, J. V.; Cui, Q.; Baboul, A. G.; Clifford, S.; Cioslowski, J.; Stefanov, B. B.; Liu, G.; Liashenko, A.; Piskorz, P.; Komaromi, I.; Martin, R. L.; Fox, D. J.; Keith, T.; Al-Laham, M. A.; Peng, C. Y.; Nanayakkara, A.; Challacombe, M.; Gill, P. M. W.; Johnson, B.; Chen, W.; Wong, M. W.; Gonzalez, C.; Pople, J. A. *Gaussian 03W*, version 6.0. Gaussian, Inc.: Wallingford CT, 2003.

(18) The pH was measured with a pH-test paper. The deuterium oxide solution was so basic that its pH seemed to be out of the range (1−11) of the test paper. From the pK_a value (9.9) of *N,N′*-dimethylethylenediamine (di-MEDA) and di-MPDA,[19] the pH value of their aqueous solutions (5 vol %) can be estimated as 11.8. In the aqueous solutions and organic solvents used here, the model compounds and the polyimines are free from protonation ($-NH_2^+-$ or $-NH^+(CH_3)-$); [20−26] In the previous[1] and present studies, therefore, the protonation has not been taken into account.

(19) Núñez, A.; Berroterán, D.; Núñez, O. *Org. Biomol. Chem.* **2003**, *1*, 2283.

(20) Smits, R. G.; Koper, G. J. M.; Mandel, M. *J. Phys. Chem.* **1993**, *97*, 5745.

(21) Borkovec, M.; Koper, G. J. M. *Macromolecules* **1997**, *30*, 2151.

(22) van Duijvenbode, R. C.; Borkovec, M.; Koper, G. J. M. *Polymer* **1998**, *39*, 2657.

(23) van Duijvenbode, R. C.; Rajanayagam, A.; Koper, G. J. M.; Baars, M. W. P. L.; de Waal, B. F. M.; Meijer, E. W.; Borkovec, M. *Macromolecules* **2000**, *33*, 46.

(24) Koper, G. J. M.; van Duijvenbode, R. C.; Stam, D. D. P. W.; Steuerle, U.; Borkovec, M. *Macromolecules* **2003**, *36*, 2500.

(25) Delpuech, J.-J.; Bianchin, B. *J. Am. Chem. Soc.* **1979**, *101*, 383.

(26) Delpuech, J.-J. Time scales in NMR: Nuclear Site Exchange and Dynamic NMR. In *Dynamics of Solutions and Fluid Mixtures by NMR.;* Delpuech, J.-J., Ed.; Wiley & Sons: New York, 1995; Chapter 3.

(27) *gNMR*, version 4.1. Cherwell Scientific Ltd: Oxford, U.K., 1995.

(28) Sasanuma, Y.; Ohta, H.; Touma, I.; Matoba, H.; Hayashi, Y.; Kaito, A. *Macromolecules* **2002**, *35*, 3748.

(29) Flory, P. J.; Mark, J. E.; Abe, A. *J. Am. Chem. Soc.* **1966**, *88*, 639.

(30) Flory, P. J. *J. Am. Chem. Soc.* **1967**, *89*, 1798.

(31) The definition of the *meso* and *racemo* forms depends on the number of bonds intervening between the nitrogen atoms, see, e.g.: Metanomski, W. V. *Compendium of Macromolecular Nomenclature;* Blackwell Science: Cambridge, MA, 1991.

(32) Abe, A.; Jernigan, R. L.; Flory, P. J. *J. Am. Chem. Soc.* **1966**, *88*, 631.

(33) The W_i matrix is common to the second through xth repeating units, these units have essentially the same $P_{m;i}$ and $p_{t;a;i}$ values. Therefore, we can adopt approximations of $P_m = P_{m;i}$ and $p_{t;a} = p_{t;a;i}$ ($i \geq 3$).

(34) Here, the last 27 elements of J^{**} are unity. If we define a 15 × 135 matrix, G_{all}, as $G_{all} \equiv G_1 (\prod_{i=1}^{x} H_i^{\alpha}) G_n$, we can obtain the z_m and $\langle r^2 \rangle_m/2$ values from $z_m = \sum_{t=1}^{27} G_{all}(1, t)$ and $\langle r^2 \rangle_m/2 = \sum_{t=109}^{135} G_{all}(1, t)$, respectively. Here, $G_{all}(1, t)$ stands for the $(1, t)$ element of G_{all}.

(35) Because z_m acts as a weight in eq 34, the $\langle r^2 \rangle$ value is largely fluctuated by low-energy chains (with large z_m's) generated accidentally. In this study, eq 35 has been adopted to evaluate $\langle r^2 \rangle$. The difference between $\langle r^2 \rangle$'s obtained from eqs 34 and 35 is at most 2%.

(36) The η interaction seems to be affected by the surrounding atomic groups. When a methyl group is in the trans position of the C−H hydrogen (e.g., in the tg^+tt conformation of tetra-MPDA), the C−H···N hydrogen bond is strengthened to $E_\eta = -0.48$ kcal mol^{-1}. When a lone pair is in the trans position of the C−H hydrogen (this rarely occurs, e.g., in the tg^+tg^+ state of tetra-MPDA), the hydrogen bond is weakened to $E_\eta = -0.09$ kcal mol^{-1}. Here, the weight-average value of $E_\eta = -0.40$ kcal mol^{-1} has been adopted.

(37) Sasanuma, Y. Intramolecular Interactions of Polyethers and Polysulfides, Investigated by NMR, Ab Initio Molecular Orbital Calculations, and Rotational Isomeric State Scheme: An Advanced Analysis of NMR Data. In *Annual Reports on NMR Spectroscopy*; Webb, G. A., Ed.; Academic Press: New York, 2003; Vol. 49; Chapter 5.

(38) Bosman, A. W.; Bruining, M. J.; Kooijman, H.; Spek, A. L.; Janssen, R. A. J.; Meijer, E. W. *J. Am. Chem. Soc.* **1998**, *120* 8547.

(39) Scherrenberg, R.; Coussens, B.; van Vliet, P.; Edouard, G.; Brackman, J.; de Brabander, E. *Macromolecules* **1998**, *31*, 456.

(40) Chai, M.; Niu, Y.; Youngs, W. J.; Rinaldi, P. L. *J. Am. Chem. Soc.* **2001**, *121*, 4670.

(41) Zacharopoulos, N.; Economou, I. G. *Macromolecules* **2002**, *35*, 1814.

(42) Jeffrey, G. A. *An Introduction to Hydrogen Bonding*; Oxford University Press: New York, 1997.

(43) Desiraju, G. R.; Steiner, T. *The Weak Hydrogen Bond: In Structural Chemistry and Biology;* Oxford University Press: New York, 1999.

(44) Tsuzuki, S.; Uchimaru, T.; Tanabe, K.; Hirano, T. *J. Phys. Chem.* **1993**, *97*, 1346.

(45) Jaffe, R. L.; Smith, G. D.; Yoon, D. Y. *J. Phys. Chem.* **1993**, *97*, 12745.

(46) Sasanuma, Y. *Macromolecules* **1995**, *28*, 8629.

MA050130Y